University of South-Eastern Norway

www.usn.no

FMH606 Master's Thesis, 2024

CO_2 Enhanced Oil Recovery in Reservoirs with Advanced Wells; Simulations and Sensitivity Analysis

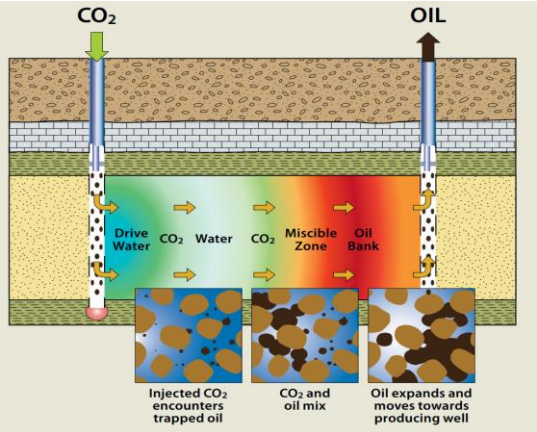

Isu Uchechukwu Agha

Faculty of Technology, Natural sciences and Maritime Sciences
Campus Porsgrunn

University of South-Eastern Norway

www.usn.no

Course: FMH606 Master's Thesis, 2024

Title: CO_2 Enhanced Oil Recovery in Reservoirs with Advanced Wells; Simulations and Sensitivity Analysis

Number of pages: 49

Student: Isu Uchechukwu Agha / 258949

Supervisors: Nora C.I. Furuvik

Soheila Taghavi Hosnaroudi

Project partner: InflowControl AS

Summary:

The global climate challenge from CO_2 emission leading to adverse climate conditions requires action to reduce its emission into the world. The process of CO_2 enhanced oil recovery is one of the actions that can contribute to reduced carbon footprints from the oil production industry. The objectives of this master's thesis are to perform a literature review on the water alternating gas (WAG), simulate a model of the miscible CO_2 injection for WAG process on computer modeling group software (CMG) and evaluate the performance of the autonomous inflow control valve (AICV) developed by InflowControl AS including sensitivity analysis of the parameters affecting the CO_2 EOR process.

The minimum miscible pressure (MMP) was determined using the CMG's-WinProp tool. The simulations were on experimental data of PVT analyses on the oil compositions and the CO_2. The CMG's-WinProp result showed that the MMP for the miscible CO_2 injection equals 15284kPa. The results from the CMG-simulations indicate that well completion with AICV can maintain good oil production while the production of water is decreased from 3e+06m^3 to 9.8e+04m^3 which corresponds to 30 times reduction in water production from the AICV completion. This is beneficial as the possibility of corrosive mixture production is avoided. In addition, the simulations of the WAG showed an increase in the oil production from 2.4e+06m^3 to 2.7e+06m^3 which is around 12.5% increase than only water injection. Furthermore, sensitive parameters such as permeability show only a small increase in the effect on oil production, while the water production is reduced with 50%. Both well perforation and the spacing show an increase in productivity of oil with increasing well distances. The simulation results also show that the vertical miscible CO_2 injection contributes to increased oil recovery compared to the horizontal miscible CO_2 injection.

Preface

This Master's thesis is the result of my research work at the University of Southeast Norway department of process technology at the faculty of technology, natural sciences, and maritime sciences. I am grateful to God almighty, my parents, and my supervisors Nora C.I. Furuvik and Soheila Taghavi Hosnaroudi for their assistance during the project.

Porsgrunn, 15.05.2024

Isu Uchechukwu Agha

Contents

Nomenclature

Abbreviation	Description	Unit
EOR	Enhanced Oil Recovery	[-]
WAG	Water Alternating gas	[-]
MMP	Minimum Miscibility Pressure	[kPa]
CMG	Computer Modelling Group	[-]
AICV	Autonomous Inflow Control Valve	[-]
ICD	Inflow Control Device	[-]
PVT	Pressure Volume Temperature	[-]
LHS	Left Hand Side	[-]
RHS	Right Hand Side	[-]
r	Radius	[m]
h	Height	[m]
g	Gravitational constant	[m/s^2]
A	Fluid flow area	[m^2]
K	Permeability	[mD]
Kg	Effective permeability to gas phase	[mD]
Ko	Effective permeability to oil phase	[mD]
Kw	Effective permeability to water phase	[mD]
Kro	Relative permeability to oil phase	[mD]
$Krocw$	Relative permeability to oil at irreducible water saturation	[-]
$Krwro$	Relative permeability to water at residual oil saturation	[-]
Krw	Relative permeability to water phase	[-]
nw	Corey coefficient for water	[-]
no	Corey coefficient for oil	[-]
S	Saturation	[fraction]
Sg	Gas saturation	[fraction]
So	Oil saturation	[fraction]

Sl	Liquid saturation	[fraction]
Sw	Water saturation	[fraction]
Sor	Residual oil saturation	[fraction]
Swc	Irreducible water saturation	[fraction]
Vg	Pore volume occupied by gas	[m^3]
Vo	Pore volume occupied by oil	[m^3]
Vw	Pore volume occupied by water	[m^3]
VT	Total pore volume in the reservoir	[m^3]
Pc	Capillary pressure	[kPa]
Pnw	Capillary pressure in the non-wetting phase	[kPa]
Pw	Capillary pressure in the wetting phase	[kPa]
Q	Volumetric fluid flow rate	[m^3/day]
dp/dx	Pressure drops over a flow length x	[kPa/day]

Greek letters	**Description**	**Unit**
Φ	Effective porosity	[fraction]
ϕa	Absolute porosity	[fraction]
ρ	Density	[kg/m^3]
μ	Viscosity of the fluid	[cP]
σ	Interfacial tension between two fluid phases	$[dynes/m]$
σnw	Interfacial tension between non-wetting and wetting fluid	$[dynes/m]$
σos	Interfacial tension between oil and surface	$[dynes/m]$
σow	Interfacial tension between oil and water	$[dynes/m]$
σws	Interfacial energy between water and surface	$[dynes/m]$
θ	Contact angle between the surface and the fluid phase	[°]

List of tables

List of figures

1 Introduction

Energy continues to be in high demand around the world. The oil and gas industry for years has played a pivotal role for the world energy production. The oil and gas will remain important sources of energy in the future. Hence, improving oil recovery with reduced carbon footprint is necessary to meet future energy demands.

The CO_2 water alternating gas enhanced oil recovery (WAG) is one of the methods used in the tertiary stage of oil production. WAG is a process of injecting CO_2 in alternating sequence with water into the oil field formation [**1**] [**2**]. Studies suggest that the injection of CO_2 into the oil field platform are beneficial for both the oil recovery and the greenhouse gas emissions. [**3**]

One example of the application of WAG EOR, is the commercial project at Lula offshore oil field, Brazil [**4**]. Compared with CO_2-EOR, the CO_2-WAG EOR gives improved displacement and sweep efficiencies [**1**]. Norway has technical potential for CO_2-WAG EOR on the North Sea oil fields. However, one problem is that the CO_2 injected can be recirculated in the producer well leading to poor distribution of CO_2 in the reservoir and can damage process equipment due to the corrosive mixture of CO_2 and water. [**5**]

Advanced wells or smart wells are used to avoid the problems with recirculation of CO_2, thus forcing CO_2 to distribute over a larger area in the reservoir. Examples of advanced well completion technologies are the autonomous inflow control valve (AICV) developed by InflowControl AS and the passive inflow control device (ICD) [**6**]. Restricting CO_2 recirculated using AICV may potentially lead to higher drawdown in high-oil saturation zones. There is also a broader contact between CO_2 and the residual oil in the reservoir, all of which will boost oil production and recovery. [**7**]

CO_2-WAG can be either miscible or immiscible depending on the minimum miscibility pressure, however this master's thesis project will investigate only the miscible process [**8**]. The producer and injector wells can either be vertical or horizontal. The CO_2-WAG performance depends on well spacing, well placing, CO_2 and water injection rates, permeability, and porosity differences in the reservoir. [**7**] [**9**] [**10**]

This thesis aims firstly at a comprehensive literature study, then secondly modelling and simulation of enhanced oil recovery for a miscible CO_2 injection with advanced wells

completed with AICV. Further performance evaluation of the AICV technology and sensitivity analysis of parameters affecting the WAG process are completed.

The Miscible CO_2-WAG with advanced wells model is developed using the commercial software Computer Modelling Group (CMG). In this project, different available modules such as Builder, FlexWell, and STARS are used to achieve the modelling and simulations. The Base case is a scenario of water injection between two producer wells. Different WAG cases are studied as well. The collected data from different simulation cases are used to perform sensitivity analysis on parameters that impact the EOR process.

2 Literature review and theory

This chapter reviews publications exploring the important parameters, mechanisms, and technological approach to enhanced oil recovery focusing on CO_2 water Alternating Gas method.

2.1 Reservoir rock and fluid properties

Reservoir rock and fluid properties are important for EOR success. The reservoir rock and fluid properties are determined by performing laboratory analyses on the cores taken from the reservoir. [**11**]

A rock which enables trapping of crude oil, natural gas and water in geological formations is often referred to as a reservoir rock. They are predominantly sedimentary rocks because they contain pores which create flow paths for accumulation and a sealing mechanism which prohibits hydrocarbon penetration to surface layers. [**12**]

Figure 2-1 shows the reservoir rock and source rock. The reservoir rock material may be composed of sandstone, limestone, or dolomite. The particles are bonded together mostly by silica, calcite, or clay [**12**]. Crude oil and natural gas are produced but not formed in the reservoir rock. Organic materials are heated and compressed for thousands of years in the source rock leading to crude oil and natural gas. [**13**]

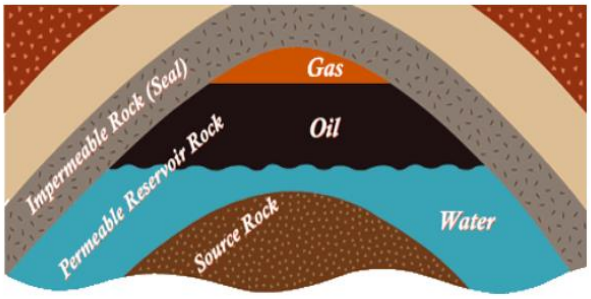

Figure 2-1 The diagram of the reservoir rock and source rock [14]

The laboratory core analyses of reservoir rock are of two categories namely routine and special analysis. The routine analyses are porosity, saturation, and permeability. The Special analyses are capillary pressure, relative permeability, wettability, and interfacial tension. [**12**] [**6**]

The primary laboratory analyses involve the measurements of the specific gravity and the gas-oil ratio. Other tests that are routinely conducted include compositional analysis of the system, constant-composition expansion, differential liberation, separator tests, and constant volume depletion while special laboratory PVT tests for very specific applications such as if a reservoir is to be depleted under miscible gas injection or a gas cycling scheme are slim-tube test and swelling test. [**20**]

2.1.1 Porosity

Porosity of a rock measures the capability of holding fluids. There are two types of reservoir rock porosity namely absolute and effective porosity. [**12**] [**13**]

The absolute porosity (Φ_a) is determined mathematically by:

$$\Phi_a = \frac{Total\ pore\ volume}{Total\ volume} \quad \text{(Equation 1)}$$

The effective porosity (Φ) is determined mathematically by:

$$\Phi = \frac{pore\ volume\ of\ interconnected\ pores}{Total\ volume} \quad \text{(Equation 2)}$$

2.1.2 Saturation

A reservoir contains three categories of fluids namely oil, water, and gas which give the total volume of a reservoir rock. Saturations are a measure of the fluid volume occupied to the total volume of the reservoir rock. [**12**] [**13**]

The total pore volume of the rock is given mathematically by:

$$V_{total} = V_{oil} + V_{water} + V_{gas} \quad \text{(Equation 3)}$$

The fluid saturation is expressed as:

$$S_{(oil,water,gas)} = \frac{Volume\ of\ (oil,water,gas)\ in\ the\ reservoir\ rock}{Total\ pore\ volume\ of\ the\ rock} \quad \text{(Equation 4)}$$

$$S_{oil} + S_{water} + S_{gas} = 1 \quad \text{(Equation 5)}$$

2.1.3 Permeability

The rock permeability controls the directional movement and the flow rate of the reservoir fluids. It measures the capacity and ability of the reservoir rock to transmit fluids. The scientist Henry Darcy mathematically expressed it as: [**12**] [**13**]

$$v = \frac{\mathrm{k\,dp}}{\mu\,\mathrm{dL}} \quad \text{(Equation 6)}$$

ν is apparent fluid flowing velocity in cm/sec, k is permeability, μ is viscosity of the flowing fluid in cp, and dp/dL is pressure drop per unit length in atm/cm.

2.1.4 Capillary pressure

Capillary pressure P_C is a phenomenon which occurs when two immiscible fluids are in contact, and it depends on the interface tension between the fluids. A discontinuity in pressure exists between the two fluids phases which are wetting P_w and nonwetting P_{nw}. Capillary pressure is expressed as: [**12**] [**13**]

$$P_C = P_{nw} - P_w \qquad \text{(Equation 7)}$$

Figure 2-2 shows an apparatus used with the restored capillary pressure laboratory technique to determine capillary pressure in a reservoir. This procedure involves saturating a core fully with the reservoir water and then placing the core on a porous membrane, which is saturated fully with water and is permeable to the water only. Pressure drop is imposed during the experiment and air is then admitted into the core chamber. The pressure is increased until a small amount of water is displaced through the porous membrane into the graduated cylinder and held constant until no more water is displaced before placing the core in the apparatus.

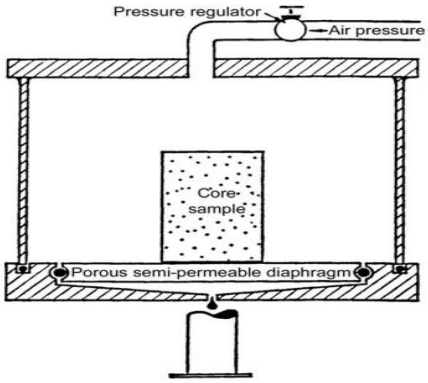

*Figure 2-2 The laboratory apparatus for capillary pressure [**12**]*

The minimum capillary pressure occurs at the largest capillary opening which is considered circular with a radius. This pressure is determined by:

$$p_c = \frac{2\sigma(cos\theta)}{r} \qquad \text{(Equation 8)}$$

2.1.5 Wettability

Wettability measures affinity for a reservoir rock to be in contact with one certain fluid phase. It influences the fluid to flow within a porous rock and impacts the distribution of the residual oil. Wettability depends on the surface roughness and varies with grain shape, grain size and roundness. [**12**] [**13**]

Figure 2-3 shows the two types of wettability occurrence in reservoir which are water-wet (left-hand-side) and oil-wet (right-hand-side). The water-wet reservoir has higher affinity for the water phase than for the oil phase and the opposite condition is the oil-wet. The contact angle between the three phases i.e. solid, liquid and gas are used to determine Wettability. The reservoir rock is water-wet if θ is below 75°, and oil-wet if θ is larger than 105°.

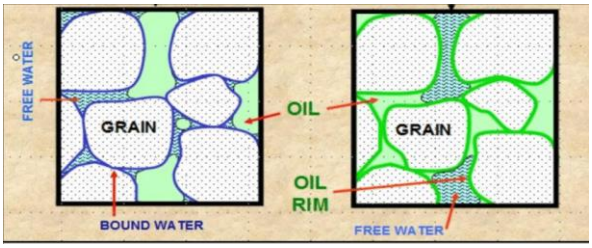

LHS RHS

*Figure 2-3 The water-wet (LHS) and oil-wet (RHS) reservoir wettability [**13**]*

2.1.6 Interfacial tension

Interfacial tension is the force which exists at the surface when immiscible fluids are in contact in the reservoir. Interfacial tension results in resisting miscibility between the fluids phases and causes changes in the spatial distribution and movement in the fluid flow within the reservoir. The interfacial tension acting at the surface is expressed as (Equation 8) [**12**]

In gas-water,

$$p_c = hg(\rho_w - \rho_g) \qquad \text{(Equation 9)}$$

In oil-water,

$$p_c = hg(\rho_w - \rho_o) \qquad \text{(Equation 10)}$$

σ is interfacial tension in dynes/cm, r is capillary radius in cm, θ is contact angle, p_c is capillary pressure in dynes/cm^2, h is capillary rise in cm, g is acceleration due to gravity in cm/sec^2, ρ_w , ρ_o , ρ_g are densities of water, oil and gas respectively in gm/cm^3.

2.1.7 Relative permeability

The relative permeability of fluid either oil, water or gas phases is the ratio of the effective permeability of that fluid to the absolute permeability of the reservoir. The sum of a multiphase component relative permeabilities is approximately unity. The effective permeability of a fluid is a function of fluid saturation and wettability. The diagram of relative permeability curve can be seen in Figure 3-4 in chapter 3. Relative permeability can be expressed mathematically as: [**12**]

$$k_{ro} = \frac{k_o}{k}\ ,\ k_{rg} = \frac{k_g}{k}\ ,\quad k_{rw} = \frac{k_w}{k} \qquad \text{(Equation 11)}$$

k_{ro} , k_{rg} , k_{rw} are relative permeabilities to oil, gas and water, k is absolute permeability, k_o , k_g , k_w are effective permeabilities to oil, gas and water for a given saturation. For a two-phase system the proposed correlations use the effective phase saturation are: [**12**]

$$S_o^* = \frac{S_o}{1-S_{wc}}\ ,\quad S_w^* = \frac{S_w - S_{wc}}{1-S_{wc}}\ ,\quad S_g^* = \frac{S_g}{1-S_{wc}} \qquad \text{(Equation 12)}$$

where S_o^* , S_w^* , S_g^* are effective oil, water, and gas saturation, S_o , S_w , S_g are oil, water, and gas saturation, and S_{wc} is connate water saturation. The relative permeabilities can be calculated analytically using Corey's method as: [**12**]

For an oil-water system:

$$k_{ro} = \left(\frac{1-S_{wc}}{1-S_{wc}}\right)^4\ ,\quad k_{rw} = \left(\frac{S_w - S_{wc}}{1-S_{wc}}\right)^4 \qquad \text{(Equation 13)}$$

For a gas-oil system:

$$k_{ro} = (1 - S_g^*)^4\ ,\quad k_{rg} = (S_g^*)(2 - S_g^*) \qquad \text{(Equation 14)}$$

2.2 EOR method of CO_2 water alternating gas (WAG)

Oil production involves three phases namely primary, secondary, and tertiary. Enhanced oil recovery, EOR is a tertiary oil production technique used for extraction of crude oil from an oil field that cannot be extracted by relying on just differential pressure. [**8**] [**13**] There are three different methods of EOR namely thermal injection, gas injection, and chemical injection. The chemical injection method involves the injection of chemicals such as surfactants, polymers, and alkalis. Gas injection method uses gases such as nitrogen gas (N_2), methane (CH_4) or carbon dioxide (CO_2) to displace crude in reservoirs. Lastly, thermal

recovery involves the introduction of heat. The aim of the three different EOR techniques is to improve mobility of oil towards the production well. [**7**] [**15**] [**16**]

CO_2 water alternating gas (WAG)-EOR is an improvement of the gas injection methods. Gases are less viscous than oil so when dissolved in oil they reduce the oil viscosity which helps to improve the mobility of the oil hence improving oil recovery. Gas injection only often comes with low sweep efficiency because of unstable displacement due to gravity segregation and viscous fingering which caused early gas breakthrough. [**1**] [**2**]

Figure 2-4 shows a diagram of a reservoir with CO_2-WAG illustration. CO_2-WAG can help to control the mobility of the gas because the water will limit fractional flow of gas which will lead to improved sweep efficiency as well as displacement efficiency. The parameters which can affect the result of CO_2-WAG are injection rates and WAG cycle length for each injection phase. [**6**] [**7**]

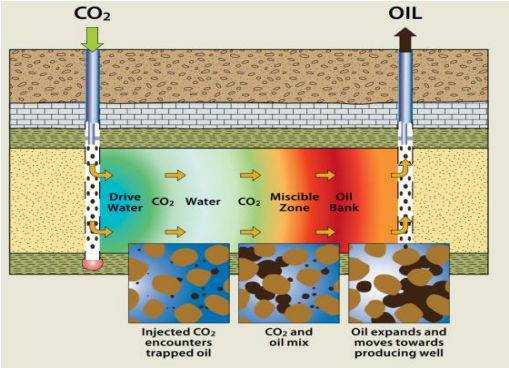

*Figure 2-4 The diagram of CO2 WAG process [**17**]*

Figure 2-5 shows an aerial view of the Bahagio studies simulation result [**1**] between CO_2-WAG (left-hand-side) and CO_2 EOR (right-hand-side) for 780 days. The CO_2-WAG reduces the gas mobility by forcing the gas to go sideways thereby sweeping more oil than the CO_2-EOR. Compared to gases such as CH_4 or N_2, the use of CO_2 is much preferable due to much lower viscosity at supercritical condition and can easily achieve miscibility which avoid less gravity segregation.

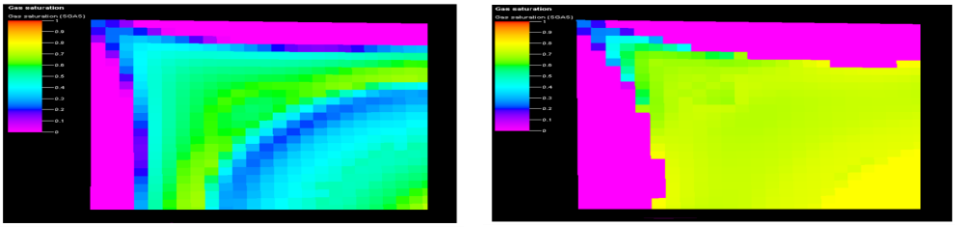

LHS RHS

*Figure 2-5 The simulation result of the WAG and CO2 EOR [**1**]*

2.3 Miscible CO_2 EOR mechanism and potentials

CO_2 EOR which occurs at a pressure equal to or higher than minimum miscibility pressure, i.e. MMP is called miscible CO_2 EOR, and below MMP is immiscible CO_2 EOR. The advantage of miscible CO_2 EOR process is that the oil volume is increased, and viscosity is lowered causing more oil to travel to the producing wells [**8**] [**18**]. MMP is the reservoir pressure above which CO_2 and oil can combine into a single-phase fluid. In Figure 2-4 miscibility between CO_2 and oil happens in the miscible zone after flooding. Mixing may occur at first contact or after multiple contacts then the lighter hydrocarbon molecules will be transferred gradually from the oil to CO_2. Attaining MMP and miscibility between CO_2 and oil is essential if the CO_2 is to act as a solvent in EOR. [**19**]

Since achieving miscibility between CO_2 and oil is the aim of a Miscible CO_2 EOR it is therefore very important to determine the minimum miscibility pressure of a reservoir. There are many experiments based on visual and non-visual information capable of determining MMP value, but three are widely used in the petroleum industry namely the conventional slim-tube tests, rising-bubble apparatus, and vanishing interfacial tension techniques. The important technical aspects of these experiments include the experimental design, operating procedure, and MMP criterion. [**20**] [**21**]

Figure 2-6 shows the experimental design setup of the conventional slim-tube tests for measuring the MMPs of various oil–gas systems. The long coiled slim tube should be saturated with the liquid phase oil sample, after which the gaseous solvent is injected at different pressures, temperatures, and injection rates to simulate the liquid–gas fluid flow in porous media. [**20**]

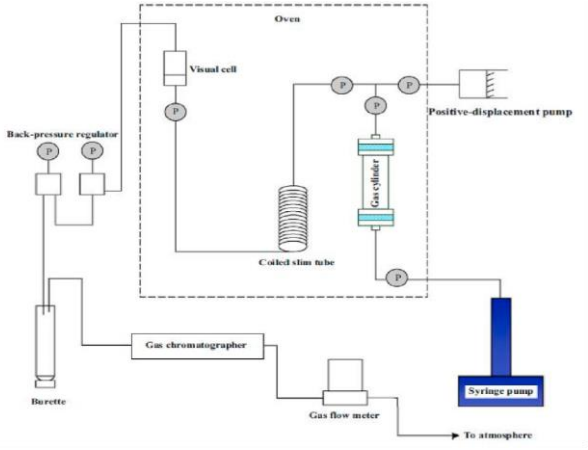

*Figure 2-6 The conventional apparatus for slim-tube test [**20**]*

The exact pressures for the experiment are difficult to ascertain but there are empirical models and correlations used to determine it range. The MMP criteria are based on the measured oil recovery factor (ORF) against injection pressure data, previous experiments suggest miscibility was achieved if the ORF of the original oil in place was over 80% at CO2-breakthrough or 94% at the end of a slim-tube test. [**22**]

2.4 Advanced wells and their impact on increased EOR

Advanced well completion is necessary in maximizing the efficiency of EOR process to avoid the common challenge of early breakthrough. Presently in the oil and gas industry advanced wells can be achieved with flow control devices, annular flow isolation, and sand control screens. [**23**]

The ICD is an example of a passive flow control device because it contains no source of electromotive force. ICD was innovated to solve the phenomena of heel to toe effect along the well because it can provide additional pressure drop to balance the pressure variation along the toe to heel of the well. The installation of ICD in wells can delay gas and water breakthrough in EOR process, but it cannot restrict the flow of unwanted effluents once a breakthrough occurs. [**23**] [**24**] [**25**]

Figure 2-7 shows a common type of ICD called the nozzle-type. During production ICDs are typically used in conjunction with screens to improve reliability. The flow characteristics of the ICD can push back against high-pressure sections to encourage flow from sections with lower formation pressure. [**23**]

*Figure 2-7 The picture of the nozzle type ICD technology [**23**]*

The AICV is an example of a reactive flow control device because it responds with a contrary course of action without direct human control when present in the well. It is a modern technology with a movable piston which acts after water breakthrough in EOR. The operating procedure of the AICV device is governed by viscosity and density differences which determines the pressure drop for different flow regimes. **[6]** [**9**] [**23**]

Figure 2-8 shows the modern AICV technology designed by InflowControl AS before it is mounted and when mounted on a well. It has a laminar flow restrictor and a turbulent flow restrictor in series which can partially or fully close the flow of fluids around them based on their viscosities. [**7**]

*Figure 2-8 The picture of the modern AICV technology designed by InflowControl AS [**26**]*

Figure 2-9 shows that if high viscous fluid like oil is around the valve (left-hand-side), the piston acts downwards which opens the valve and if low viscous fluids like CO_2 or water (right-hand-side) is around the valve, the piston acts upwards which closes the valve. **[6]** [**7**]

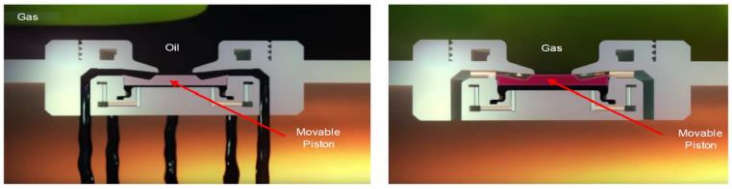

LHS RHS

Figure 2-9 The picture of the AICV movable valve when open (LHS) and close (RHS) [7]

2.4.1 Comparison between AICV and ICD

Figure 2-10 shows the result from an investigative study of the performance of ICD against AICV. Taghavi et al. [**7**] compared the ICD with the AICV performance and suggest that both have the same strength toward pressure drop when the volumetric flow is 1 m^3/h, but there is significant gas and water reduction by using AICV under the same conditions. However, when the volumetric flowrate is increased the AICV provides more pressure drop.

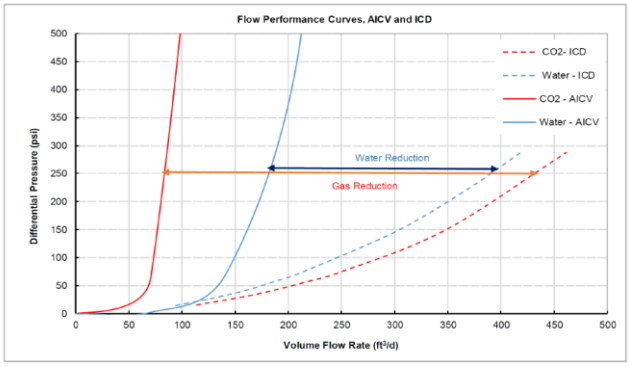

Figure 2-10 The performance graph of pressure and volumetric flowrate for AICV and ICD [7]

2.5 CO_2 and reservoir fluids characteristics

Reservoirs in the petroleum industry are classified as dry gas, wet gas, gas condensate, volatile oil, and black oil. The fluid composition includes nonhydrocarbons, hydrocarbon, and water. The nonhydrocarbons are N_2, CO_2, and H_2S, the hydrocarbons are C_1, C_2, C_3, iC_4, nC_4, iC_5, nC_5, C_6, and C_{7+} and the water is usually a brine consisting mostly of sodium chloride (NaCl). [**12**]

The characterization of fluids and CO_2 is important to achieve successful CO_2 EOR and sequestration, this is because the distribution of fluids in the reservoir is dependent on characteristics as well as other forces that drives fluid movement for example gravity, capillary, molecular diffusion, thermal convection, and fluid pressure gradients. **[8]** [**12**]

2.5.1 CO_2 behavior

The physicochemical properties of CO_2 suggest it is odorless, colorless, and inflammable. CO_2 is naturally present in most reservoirs as a fluid composition. However, the abundant presence of anthropogenic CO_2 in the earth crust is harmful and can be mitigated through carbon capture utilization and storage (CCUS). [**3**]

Figure 2-11 is the pressure-temperature (PT phase) diagram generated by PVTsim which illustrates that CO_2 can exist in solid, liquid, gas, and supercritical phase conditions. The plot shows that CO_2 is in supercritical state at pressure around 399bara and temperature of 40°C. In EOR, the phase condition of importance is the supercritical condition of CO_2 due to the immobile nature of the oil in the residual oil zones. Supercritical CO_2 has a density around 0.6-0.8 g/cm^3. These properties at supercritical condition make it very useful for extraction purposes. [**27**] [**28**]

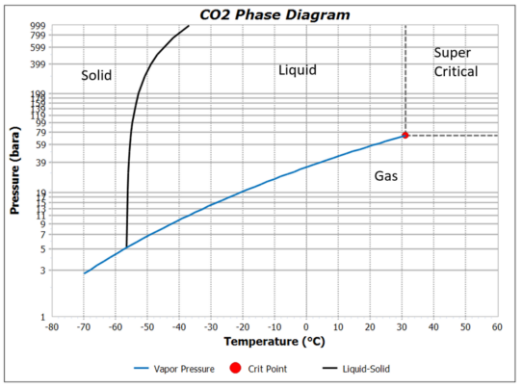

*Figure 2-11 The pressure-temperature phase diagram of CO_2 [**28**]*

In the EOR process, the residual oil zone is usually at depth >1200m therefore supercritical phase condition for CO_2 is easily achieved due to the high pressures and temperatures at this depth. The oil will be miscible with supercritical CO_2, then the oil viscosity and Interfacial tension reduces when swelling occurs due to solubility of CO_2 in oil. These occurrences will promote good oil mobility. [**17**]

Figure 2-12 shows the study result from an EOR simulation. A pressure-temperature phase envelope from swelling of reservoir oil and CO_2 mixture when 100, 200 and 300 mol% CO_2 is injected into a reservoir. [**28**]

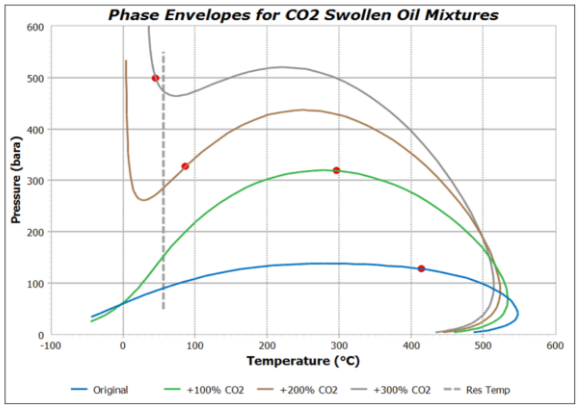

*Figure 2-12 The swollen CO_2 P-T phase envelope from simulation study [**28**]*

Another effect is that CO_2 dissolved in water can form corrosive acid with calcite component presence in the rock. The chemical equation below expressed the reaction: [**29**]

$$H_2O + CO_2 + CaCO3 \rightarrow Ca(HCO_3)_2$$

This phenomenon will affect the reservoir wettability and relative permeability characteristics making the rock more water wet which favors oil displacement efficiency. [**11**] However, there are economic challenges after breakthrough if this corrosive mixture leaves the producer wells because the process equipment on the platform will be endangered. [**17**]

3 Model development on CMG

This chapter gives a detailed explanation of the steps taken to create the reservoir rock, reservoir fluid and wellbore for the model using suite packages such as WinProp, Builder, Stars and FlexWell in the Computer Modelling Group (CMG) 2023.10 general release software version.

3.1 Reservoir fluid components and characterization

The WinProp package is capable of fluid characterization, matching experimental data, and constructing phase diagrams such as pressure-volume-temperature PVT using equation of states such as Peng-Robinson with data obtained from laboratory analysis of reservoir samples. However, the aim of the created fluid model in this work is to calculate the minimum miscibility pressure MMP required to achieve miscibility between oil and CO_2 injected. It was determined to be 15284 kPa at reservoir temperature of 85.5°C.

Figure 3-1 shows the pressure-temperature phase envelope of CO_2 generated by WinProp. The two-phase boundary is the green curve, and the critical temperature and pressure are approximately 6500kPa and 425°C.

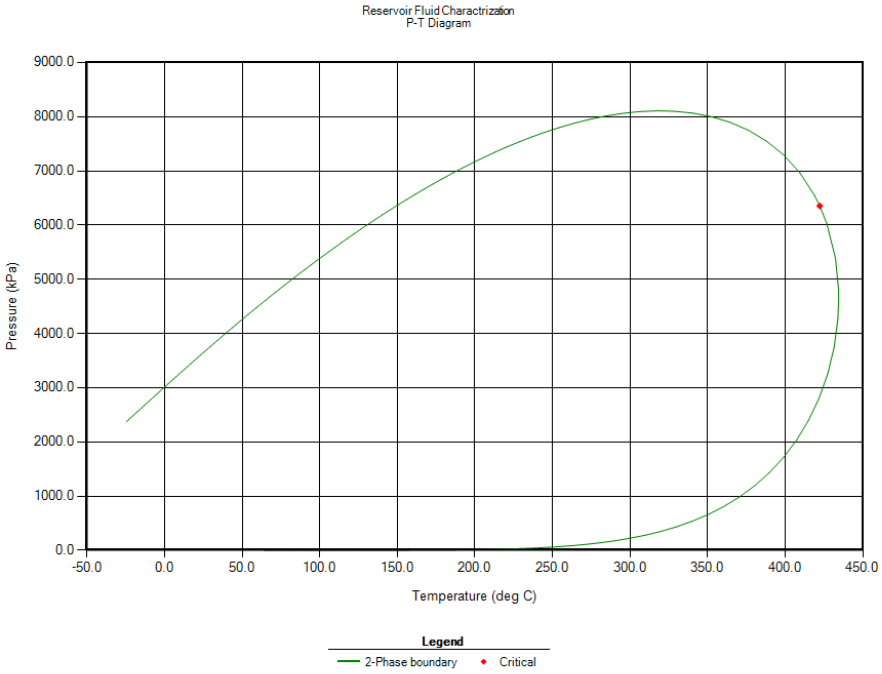

Figure 3-1 The P-T phase envelope of CO_2 created in WinProp

There are seven components in the oil phase and water in the aqueous phase created on WinProp for the reservoir fluid components.

Table 3-1 below gives an overview of the mass fraction of the different compositions in oil phase primary present in the reservoir as specified in WinProp.

Table 3-1 The mass fractions of compositions in oil phase

Component	Mass fraction
CO2	1.18
N2toCH4	11.70
C2H6_NC4	19.45
IC5toC07	22.03
C08toC12	28.15
C13toC19	9.39
C20_C30+	8.09
Sum	100.00

Table 3-2 gives the oil phase compositions properties such as molar density, molecular weight, and viscosity of the rock fluids specified in WinProp at the initial conditions of the reservoir. These values were obtained from CMG default for these components values.

Table 3-2 The liquid phase properties of the rock fluid compositions

Component	Molar density	Molecular weight	Viscosity
	mol/m3	kg/mol	cp
C20_C30+	2716.55	0.48	0.17
CO2	19009.50	0.05	0.42
N2toCH4	20743.20	0.01	0.25
C2H6_NC4	13624.90	0.05	0.32
IC5toC07	11067.70	0.08	0.33
C08toC12	5293.12	0.12	0.34
C13toC19	2645.88	0.21	0.25

3.2 The reservoir

One homogeneous reservoir and one heterogeneous reservoir were designed in builder suite package with cartesian plane. For both reservoirs, there are ten (10) grids in the I-J direction, and fifteen (15) in the K direction. The length, width and height dimensions of the reservoir are 300m, 500m and 150m. The top of the reservoir is at a depth of 1000m and the bottom of the reservoir of the reservoir is at depth 1150m. Most properties of the reservoirs were left in the original preset initial values specified by CMG, however both reservoirs porosity was modified to 0.35, other properties modified for the reservoirs are constant temperature of 85.5°C and a varying pressure of 22000 kPa and 20000 kPa at the top and bottom depth respectively to ensure sufficient drive force. The reference pressure was modified to 20684.3 kPa, the value was set much higher than MMP to ensure the process remains a miscible CO_2 process, the surface pressure condition was 101 kPa and the surface temperature condition was 16.85°C.

Figure 3-2 shows the pictorial view of the homogeneous reservoir (left-hand-side) and heterogeneous reservoir (right-hand-side). The homogeneous reservoir permeability is constant all through the layers at 2500mD. The heterogeneous reservoir permeability varies from 2500mD to 10000mD.

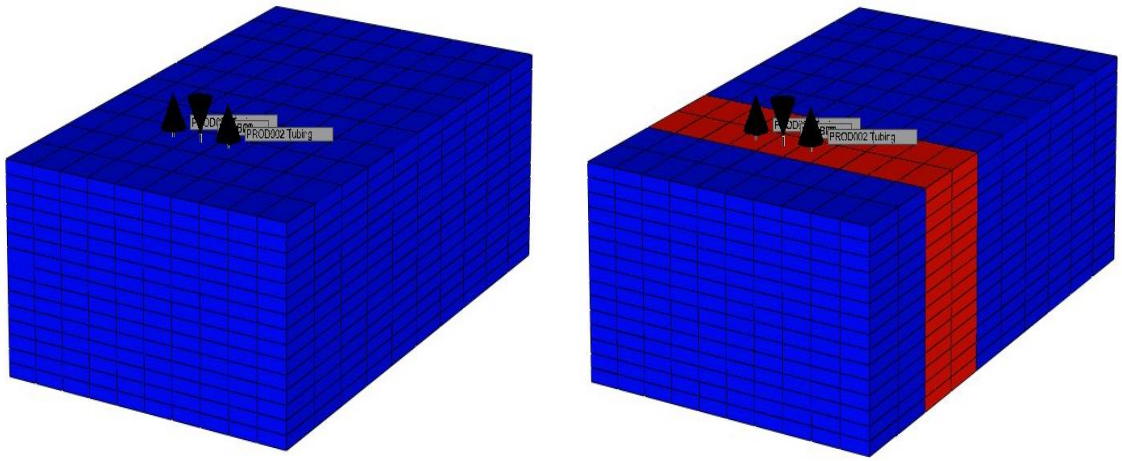

LHS RHS

Figure 3-2 The 3-D view of the homogeneous (LHS) and heterogeneous reservoir (RHS)

Figure 3-3 shows the highest permeability region for the heterogeneous reservoir was placed on the heel section of the producer wells to aid the mobility of reservoir fluid through the producer wells.

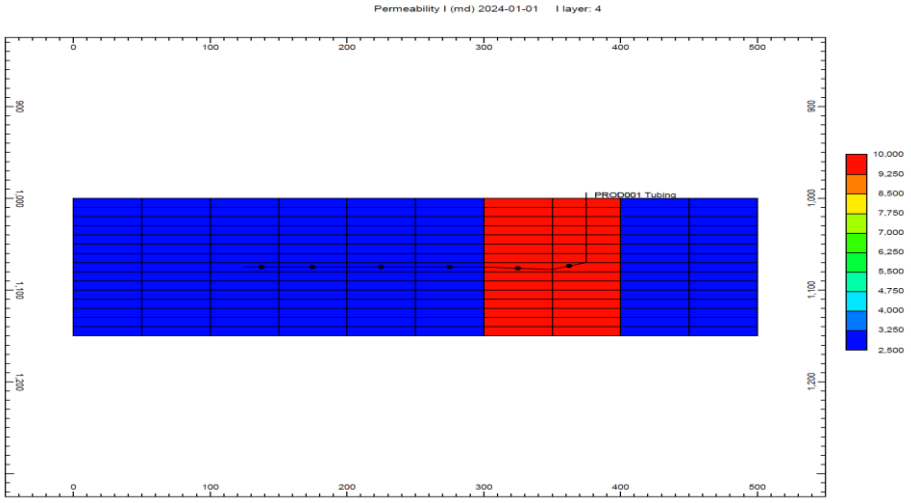

Figure 3-3 The 2-D view of the producer well of the heterogeneous reservoir

The wettability state of the rock is water wet. The relative permeability curves datasets were calculated based on the Stone II model for two-phase. Figure 3-4 shows the relative permeability curves generated in builder for the oil-water phase with respect to water saturation, and for the gas-liquid phase with respect to liquid saturation. In the relative permeability curve of the oil-water phase (left-hand-side), the red curve is oil, and the blue curve is water. The oil is immobile below 0.25 saturation, and the water maximum saturation is 0.78. In the relative permeability of gas-liquid phase with respect to liquid saturation (right-hand-side), the red curve is gas, and the blue curve is oil. The connate water plus residual oil saturation is 0.55 and the residual oil is 1.

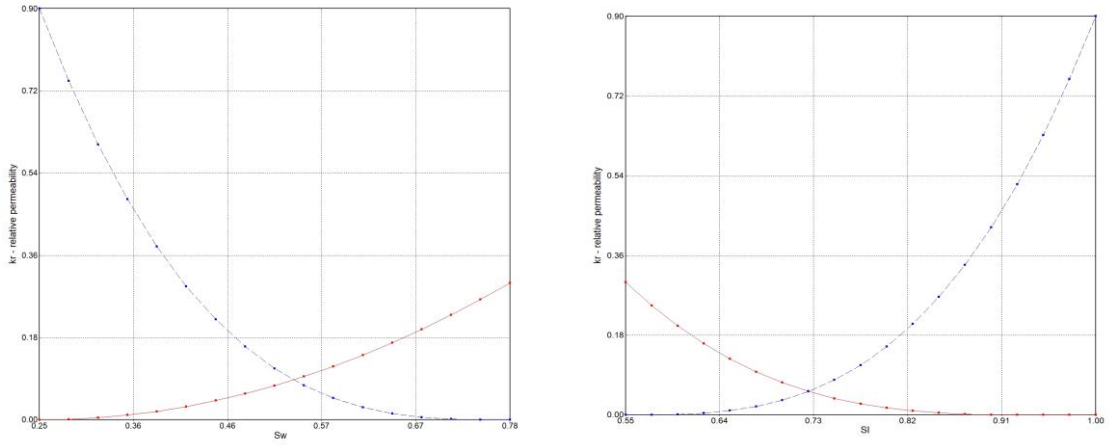

LHS RHS

Figure 3-4 The water-wet relative permeability curves for the oil-water phase (LHS) and the gas-oil phase (RHS)

3.3 The simulation cases

Several simulations were conducted for different models developed to check sensitivity analysis. The cases were based on homogeneous reservoir labelled as Case-A and heterogeneous reservoir as Case-B. Additional model cases were developed firstly based on injection fluid such as water EOR and WAG. Secondly, based on wellbore placement such as horizontal and vertical wells. Thirdly, based on wellbore completion with and without AICV. Further investigations were made into the effect of parameters such as well spacing and permeability. Table 3-3 gives an overview of all simulated model cases.

Table 3-3 The simulated model cases for case-A and case-B on CMG

		Injection Mode		Well Placement		AICV
		Water	WAG	Horizontal	Vertical	
Homogeneous						
	Case-A-1		✓	✓		✓
	Case-A-2		✓	✓		
	Case-A-3		✓		✓	✓
	Case-A-4		✓		✓	
	Case-A-5	✓		✓		✓
	Case-A-6	✓		✓		
	Case-A-7	✓			✓	✓
	Case-A-8	✓			✓	
Hetrogeneous						
	Case-B-1		✓	✓		✓
	Case-B-2		✓	✓		
	Case-B-3		✓		✓	✓
	Case-B-4		✓		✓	
	Case-B-5	✓		✓		✓
	Case-B-6	✓		✓		
	Case-B-7	✓			✓	✓
	Case-B-8	✓			✓	

3.3.1 Duration of simulation and well placement

The timeline of the simulated cases was for ten (10) years from the period of 2024-01-01 to 2034-01-01. The base case is the water injection from an injector well and two producer wells open for production throughout all the years in the simulation period, the injector well was perforated at the middle between two producers wells. The WAG case involves the same

wells and same perforation location as the base case, but the injection cycle period was modified to have injection period for water and CO_2.

Figure 3-5 shows an illustration of the timeline for the WAG with continuous production. The annulus of the producer well is shut but the tubing is open.

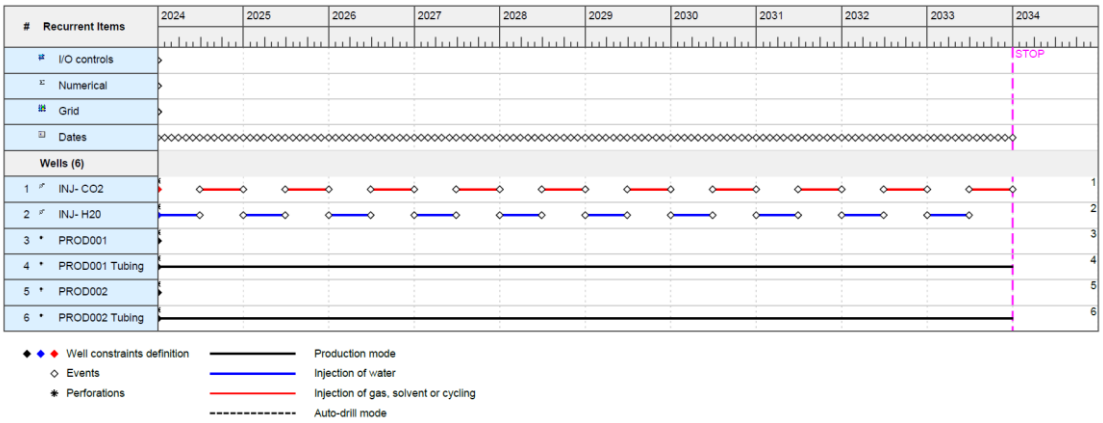

Figure 3-5 The timeline of WAG fluid injection and production cycle periods

The wells developed in builder were horizontally in J-direction and vertically in K-direction. For the AICV completion on the producer wells, flexwells were created on the existing producer wells to have anulus and tubing with FCD tables on the packers. Parameters such as conductivities, heat capacity, heat loss etc. were left in the CMG default values, but the wall inner and outer diameters were modified to 0.3 and 0.35.

Table 3-4 below shows the type of constraint and the specified values for the simulations. The injector well and producer well-1 and producer well-2 for both the horizontally and vertically perforations have same constraints values specified except STL surface liquid rate.

Table 3-4 The constraint specification for both the injector well and producer wells

	Constraint Type	Limit	Value	Action	Well Placement
Injector					
	BHP bottom hole pressure	MAX	22000 kPa	Continue	Horizontal & vertical
	STG surface gas rate	MAX	50000 m3/day	Continue	Horizontal & vertical
	STW surface water rate	MAX	10000 m3/day	Continue	Horizontal & vertical
Producer					
	BHP bottom hole pressure	MIN	15000 kPa	Continue	Horizontal & vertical
	STL surface liquid rate	MAX	840 m3/day	Continue	Horizontal
	STL surface liquid rate	MAX	200 m3/day	Continue	Vertical

Figure 3-6 shows a picture of the horizontal wells from the I-J direction view. The producer well-1 is at the left, injector well is at the middle, and producer well-2 is at the right.

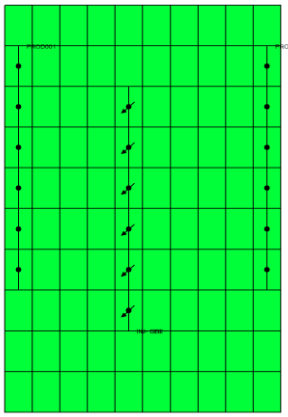

Figure 3-6 The I-J direction view of the horizontal placement of the injector and producer wells

Figure 3-7 shows the picture of the horizontal producer well-1 from the J-k direction view.

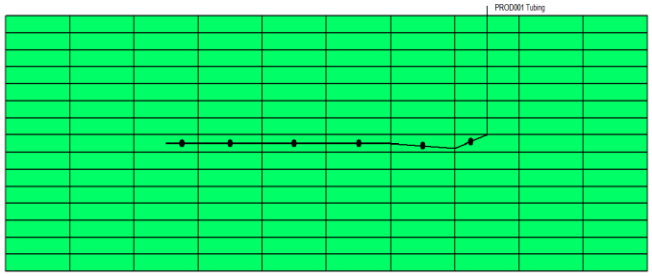

Figure 3-7 The J-K direction view of the horizontal producer well-1

Figure 3-8 shows the picture of the vertical wells from the I-k direction view. The producer well-1 is at the left, injector well is at the middle, and producer well-2 is at the right.

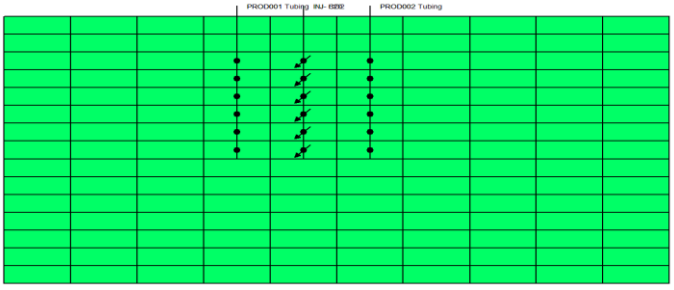

Figure 3-8 The I-K direction view of the vertical placement of the injector and producer wells

4 Results and discussion

In this chapter there are five subchapters where the results from the simulation cases are presented in order to investigate some sensitive parameters. The WAG EOR process was compared with water injection in subchapter 4.1. The performance of AICV well completion in terms of cumulative production for oil and water is presented in subchapter 4.2. The impact of reservoir permeability on oil production in WAG EOR was investigated by comparing homogeneous reservoir to heterogeneous reservoir in subchapter 4.3. In subchapter 4.4 the injector well position of Case A-2 was modified to investigate the impact on productivity, also the effect of well spacing on productivity was investigated. The well placement was investigated by comparing horizontal well and vertical well in subchapter 4.5.

4.1 Comparison of WAG and water injection

In this subchapter, the resulting effect of injecting CO_2 alternately with water was carried out by comparing the field groups results for horizontal wells with AICV at the end of the simulation period in the year 2034 at standard conditions.

Figure 4-1 shows the graph of the field oil rate of the two producer wells at standard condition. The thick green line represents Case-A-5 i.e. the water injection, and the dash green line represents Case-A-1 which is the WAG.

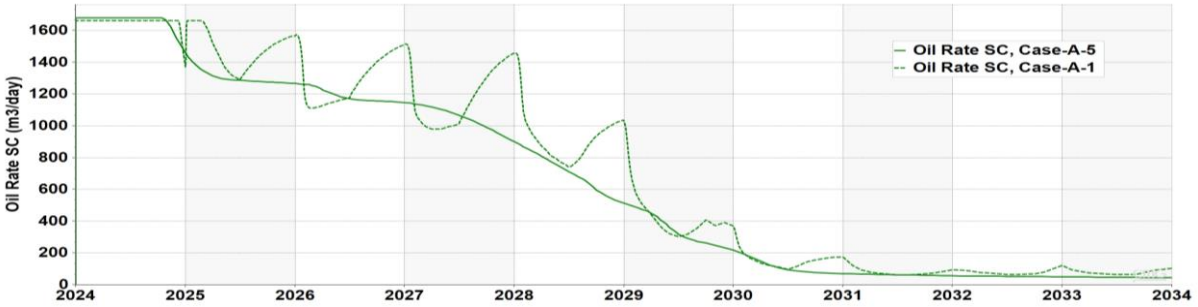

Figure 4-1 The field oil rate of the two producer wells at standard condition for case-A-1 and case-A5

The field oil rate in Figure 4-1 illustrates that both WAG and water injection can promote oil productivity. The case-A-1 has an oscillating curve because the highest peaks in the oil production appear during the CO_2 injection period. This is because if CO_2 is well circulated around the reservoir region of high oil saturation, the mobility of the oil toward the producer wells increases.

Figure 4-2 shows the graph of the field cumulative oil of the two producer wells at standard condition. The thick green line represents Case-A-5 i.e. the water injection, and the dash green line represents Case-A-1 which is the WAG.

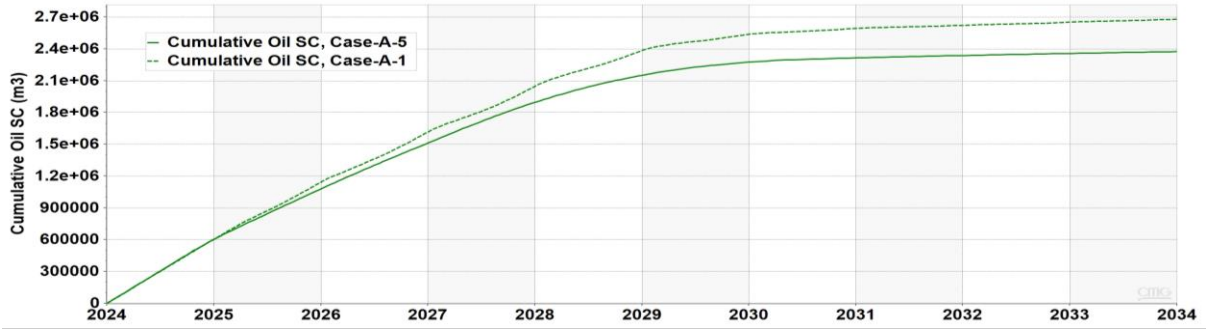

Figure 4-2 The field cumulative oil of the two producer wells at standard condition for case-A-1 and case-A-5

In year 2034, the WAG produces more oil at 2.7e+06m^3 in Figure 4-2 because CO_2 injection into the reservoir gave a higher yield boost which is around 12.5% increase in the oil production compared to case-A-5 where the oil cumulative production is 2.4e+06m^3.

Figure 4-3 shows the graph of the field cumulative water of the two producer wells at standard condition. The thick blue line represents Case-A-5 i.e. the water injection, and the dash blue line represents Case-A-1 which is the WAG.

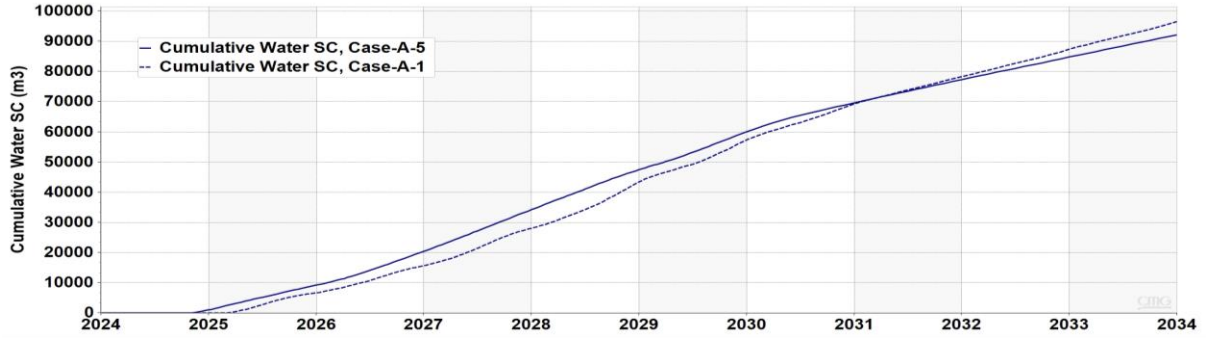

Figure 4-3 The field cumulative water of the two producer wells at standard condition for case-A-1 and case-A-5

The WAG has a more delayed water breakthrough at the early period of year 2025 which is good because early recirculation of water in the producer wells leads to poor sweeping of the oil. Cumulatively, the WAG case produces more water at 9.8e+04m^3.

Figure 4-4 shows the graph of the well bottom hole pressure of the producer well-1 which is the same as the producer well-2 because the well constraints are the same. The thick red line represents Case-A-5 i.e. the water injection, and the dash red line represents Case-A-1 which is the WAG.

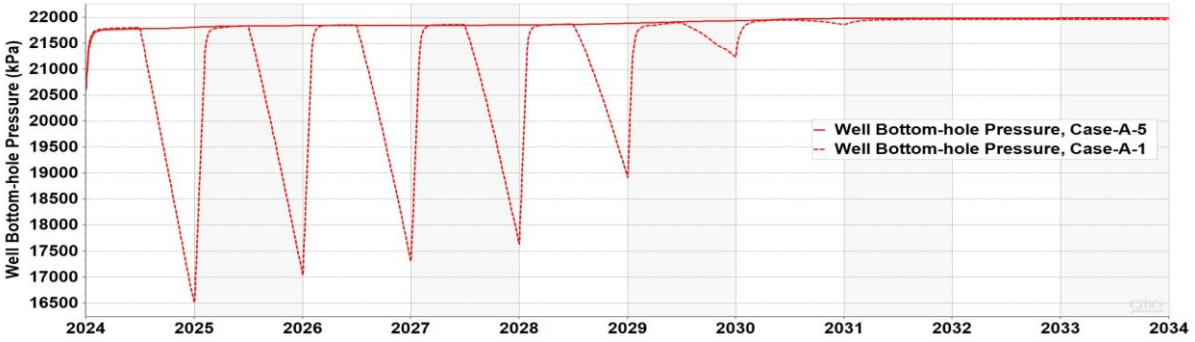

Figure 4-4 The graph of the well bottom hole pressure of the producer well-1

The water injection is capable of oil production because in Figure 4-4 the water injection into the reservoir helps maintain the pressure in the reservoir close to the maximum bottom hole pressure constraint of 22000kPa which assist the mobility of oil to the producer wells. However, the WAG process has an increased drawdown in the pressure at periods when CO_2 is injected which is good for more oil mobility and increased productivity.

Figure 4-5 shows the result of the oil saturation in the j-k direction view at the injector well perforation in the year 2034 for the WAG (left-hand-side) and the water injection (right-hand-side).

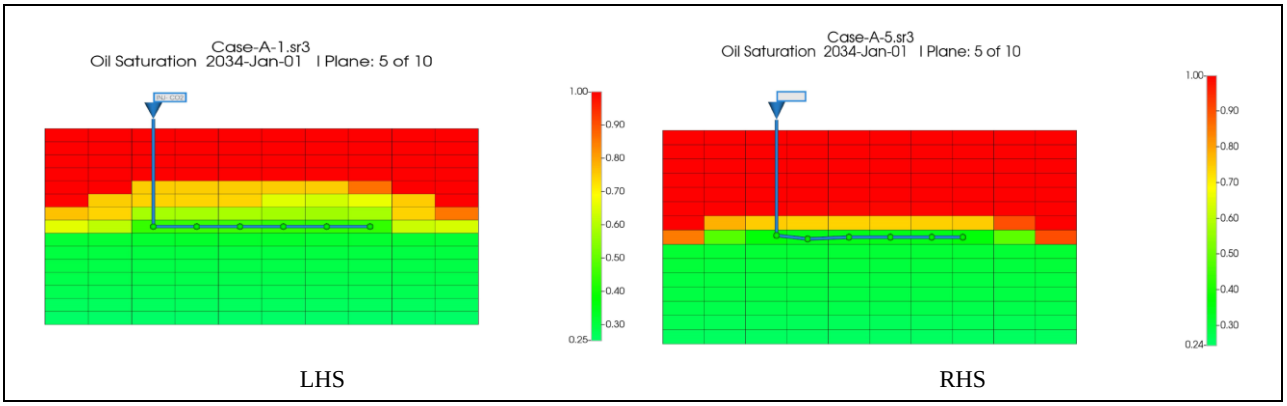

Figure 4-5 The reservoir oil saturation for the WAG (LHS) and the water injection (RHS)

Oil saturation is an important parameter to observe when comparing WAG and water injection. Figure 4-5 indicates that WAG removes more oil than water injection. In Figure 4-5 the green color zones in the reservoir are where oil have been removed and replaced with water. The scaling shows that the red color zone is the high oil saturation zone and has a mole fraction of 1

which means oil is the only component present. The orange and yellow color indicates two-phase zone of oil and water. The water-wet irreducible zone of oil is at 0.25 meaning below the value oil has no mobility

Figure 4-6 shows the result of the water saturation in the j-k direction view at the injector well perforation in the year 2034 for the WAG (left-hand-side) and the water injection (right-hand-side).

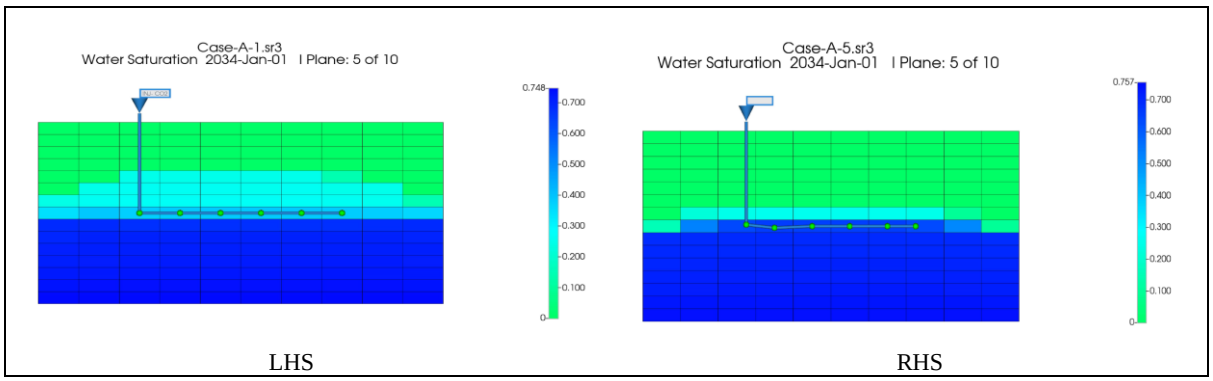

Figure 4-6 The reservoir water saturation for the WAG (LHS) and the water injection (RHS)

In Figure 4-6 more water is present in WAG at year 2034 than water injection. It is important to note that the green color zones are the are remaining oil, and the deep blue color zones are water in the reservoir. The lighter blue color refers to a two-phase zone of oil and water.

4.2 The performance of AICV

This subchapter investigates the performance of autonomous inflow control valve (AICV) by studying the simulation results of the field cumulative oil and water production at standard condition of Case-A-1 which has AICV completion on the horizontal producer wells and Case-A-2 which has no AICV completion.

Figure 4-7 shows the graph of the field cumulative oil of the two producer wells at standard condition. The thick green line represents Case-A-1 i.e. with AICV, and the dash green line represents Case-A-2 which is without AICV.

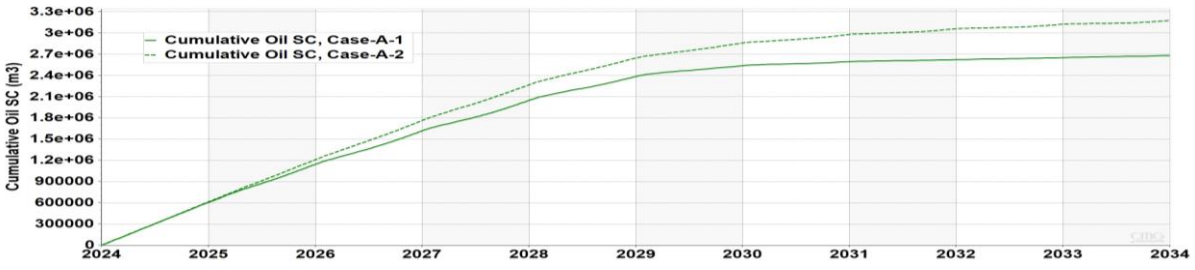

Figure 4-7 The field cumulative oil of the two producer wells at standard condition for case-A-1 and case-A-2

The AICV shows a fantastic performance over a well completion without it. From Figure 4-7, we can see that the no AICV case produces more oil at 3.3e+06m^3, and the AICV produces 2.7e+06m^3. The no AICV result may contain a 2-phase mixture of oil with unwanted water. Oomole and Osoba [**29**] cited that "water can form corrosive mixture with CO_2". Hence the goal is to produce as little water as possible to avoid this occurrence because corrosive mixture is not suitable for the top side facilities. This is observed from Figure 4-8, the cumulative water produced is 30 times lower at 9.8e+04m^3 compared to 3e+06m^3 of no AICV at year 2034. This is because the inflow from the reservoir is non-uniform along the wellbore with AICV completion resulting in choking of unwanted water production.

Figure 4-8 shows the graph of the field cumulative water of the two producer wells at standard condition. The thick blue line represents Case-A-1 i.e. with AICV, and the dash blue line represents Case-A-2 which is without AICV.

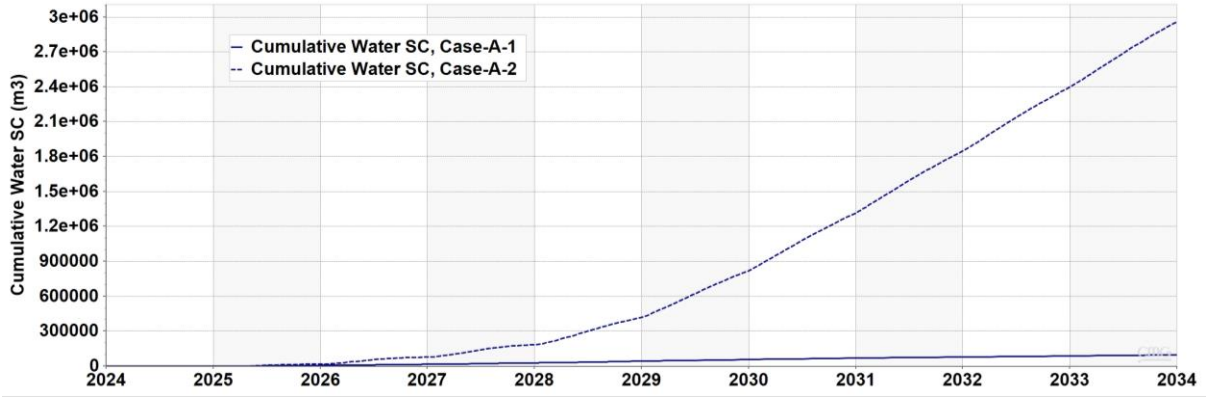

Figure 4-8 The field cumulative water of the two producer wells at standard condition for case-A-1 and case-A-2

4.3 Comparison of homogeneous and heterogeneous reservoir

The effect of permeability on reservoir productivity is the main aim of this subchapter. This was achieved by comparing the productivity results of the homogeneous reservoir with that of heterogeneous reservoir which were both built in chapter 3.

We see from Figure 4-9 and Figure 4-10 that permeability of the reservoir plays an important role in productivity of oil and water. When the permeability was increased in the heterogeneous reservoir from 2500mD to 10000mD around the heel section of the wells, there was very slight increase in the cumulative oil production in the year 2034 from 2.65e+07m^3 to 2.7e+07m^3.

Figure 4-9 shows the graph of the field cumulative oil of the two producer wells at standard condition. The thick green line represents Case-A-1 i.e. homogeneous reservoir, and the dash green line represents Case-B-1 which is the heterogeneous reservoir.

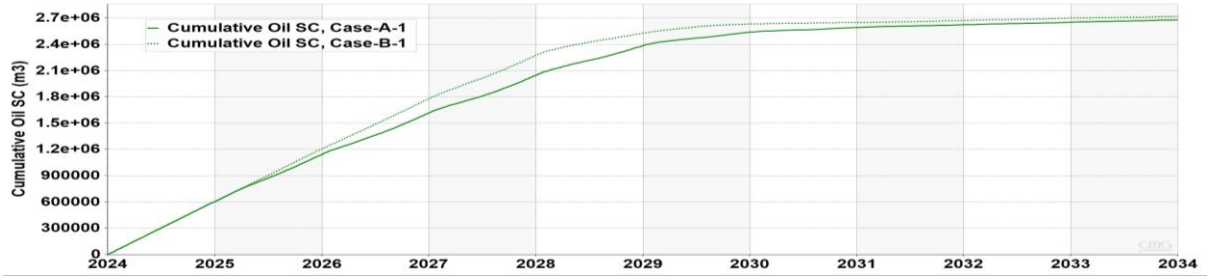

Figure 4-9 The field cumulative oil of the two producer wells at standard condition for case-A-1 and case-B-1

Figure 4-10 shows the graph of the field cumulative water of the two producer wells at standard condition. The dash blue line represents Case-A-1 i.e. homogeneous reservoir, and the thick blue line represents Case-B-1 which is the heterogeneous reservoir. The heterogeneous reservoir benefits the goal of producing less water because the cumulative water produced in the year 2034 is 5.2e+04m^3, which is around 50% reduction in the homogeneous reservoir value of 9.8e+04m^3.

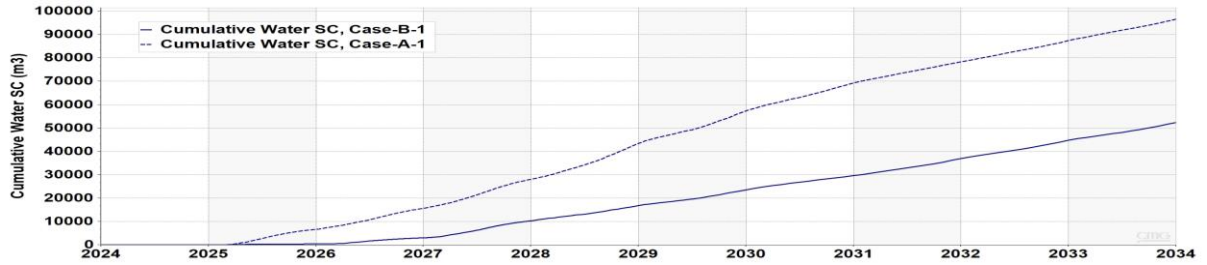

Figure 4-10 The field cumulative water of the two producer wells at standard condition for case-A-1 and case-B-1

4.4 The impact of well spacing and position on production

This subchapter focuses on the productivity effect of the wells perforation location and the spacing between the wells. The Case-A-2, a case of horizontal WAG with no AICV was modified by changing the injector perforation location from middle to the right-hand side as shown in Figure 4-11 below.

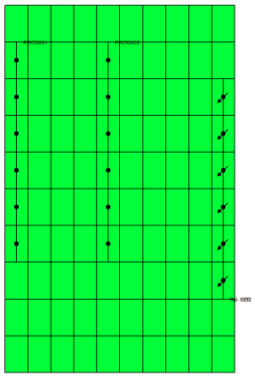

Figure 4-11 The case-A-2 injector well perforation changed from to the right-hand side

Different perforation locations of wells have significant impact on the productivity of oil and water, so there is need to find the best positions for the wells which will achieve maximum oil productivity from the reservoir. From Figure 4-12, we see that the oil rate curve pattern with respect to the timeline is very similar despite change in perforation location of the injector well, but however there is increase in the oil production rate with the injector well at the right-hand-side.

Figure 4-12 shows the graph of the field oil rate of the two producer wells at standard condition. The dash green line represents Case-A-2 with injector well in the middle, and the dash red line represents Case-A-2 with injector well at the right-hand side.

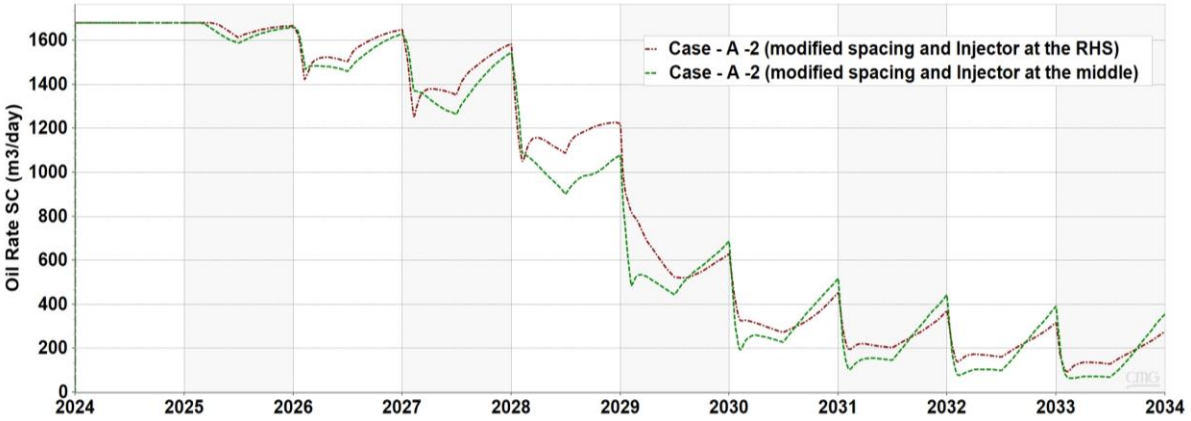

Figure 4-12 The field oil rate of the two producer wells at standard condition for modified case-A-2

Figure 4-13 shows the graph of the cumulative oil of the two producer wells at standard condition. The thick red line represents Case-A-2 with injector well in the middle, and the thick green line represents Case-A-2 with injector well at the right-hand side. At year 2034, the cumulative oil of the injector well at the right-hand side is 3.3e+06m^3, and the injector well at the middle cumulative oil is 3.1e+06m^3.

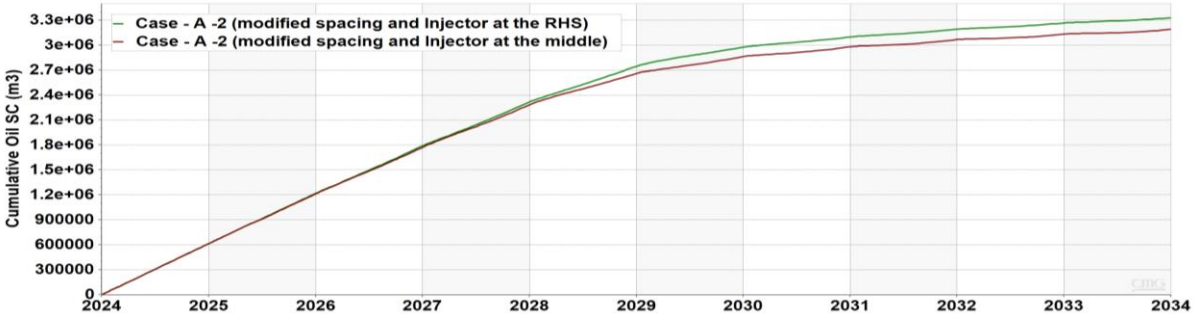

Figure 4-13 The field cumulative oil volume of the two producer wells at standard condition for modified case-A-2

Figure 4-14 shows the graph of the cumulative oil of the two producer wells at standard condition. The dash blue line represents Case-A-2 with injector well in the middle, and the thick blue line represents Case-A-2 with injector well at the right-hand side. When injector well is at the right-hand-side cumulative water is 2.8e+06m^3, and when injector well is at the middle cumulative water is 3.0e+06m^3.

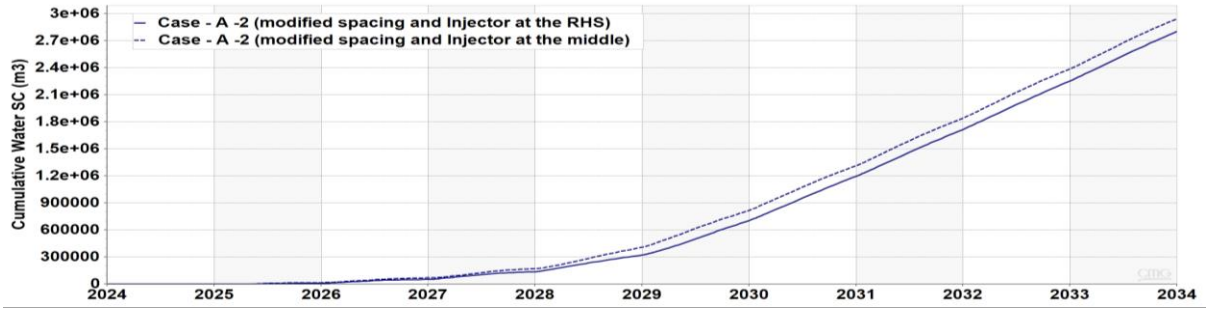

Figure 4-14 The field cumulative water volume of the two producer wells at standard condition for modified case-A-2

The Case-A-2 producer wells were then modified to have less distance from the injector well as shown in Figure 4-15 below.

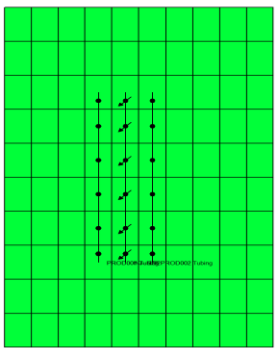

Figure 4-15 The modified case-A-2 with less well spacing distances

From Figure 4-16 and Figure 4-18 it is important to avoid the producer wells been too close to the injector well, this is because we observed an early water breakthrough at the start of the WAG. Possibly because the injected fluid (water) at the start of every year is being produced directly in the producer well instead of distributing around the reservoir. This effect brings down the oil rate in Figure 4-16 close to zero in the oscillating curve at the start of every year which were periods when water was injected.

Figure 4-16 shows the resulting effect of these changes on the graph of the field oil rate of the two producer wells at standard condition.

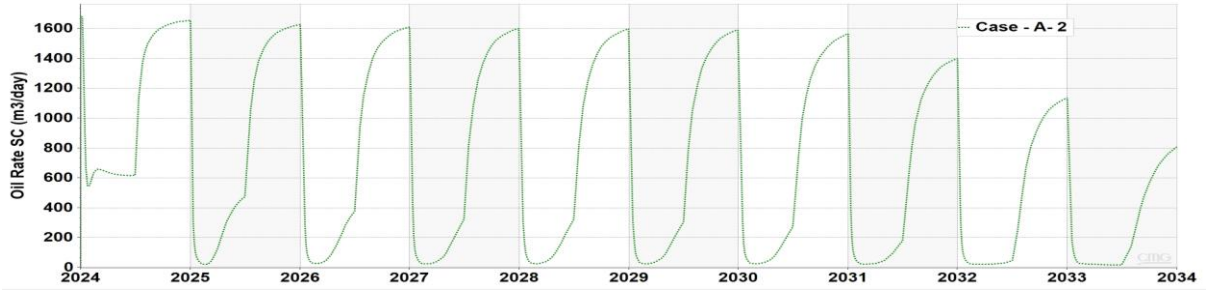

Figure 4-16 The field oil rate for the modified case-A-2 with less well spacing distance

Figure 4-17 shows the resulting effect of these changes on the graph of the field cumulative oil of the two producer wells at standard condition. We noticed a reduced cumulative oil to 2.7e+06m^3 compared to Figure 4-13 where it was 3e+06m^3. This is because of a lower sweeping efficiency from poor distribution of CO_2 and water.

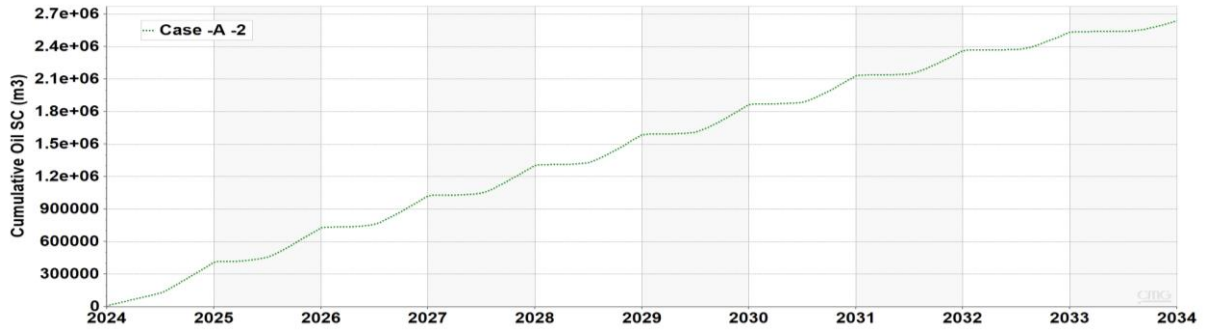

Figure 4-17 The field cumulative oil volume for the modified case-A-2 with less well spacing distance

Figure 4-18 shows the resulting effect of these changes on the graph of the field cumulative water of the two producer wells at standard condition. At year 2034, The cumulative water produced initially 3e+06m^3 in Figure 4-14 to 3.5e+06m^3, this is because of early breakthrough at the beginning of year 2024.

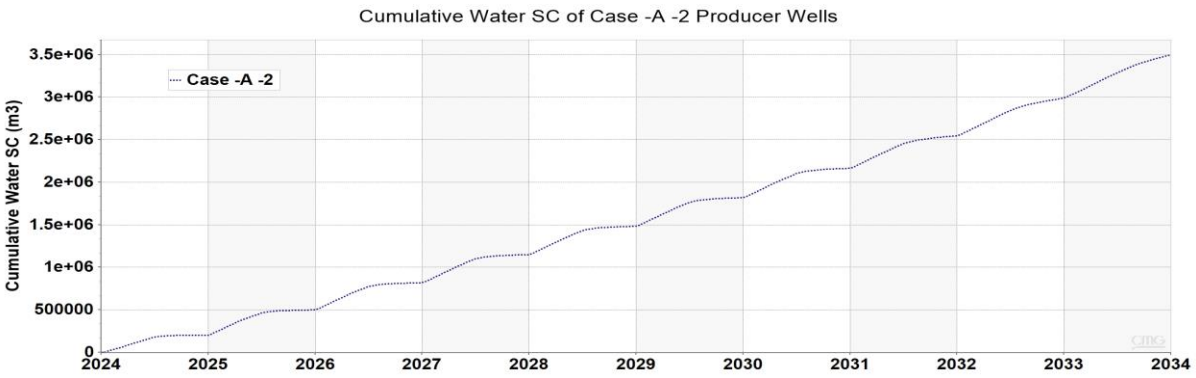

Figure 4-18 The field cumulative water volume for the modified case-A-2 with less well spacing distance

4.5 Comparison of horizontal and vertical wells

This subchapter focuses on the impact of well placement on miscible CO_2 injection base on productivity. The comparison is between vertical injector well with vertical producer wells, and horizontal injector well with horizontal producer wells. This comparison was done for cases with AICV and cases without AICV. The constraints for the producer wells of vertical and horizontal were adjusted in terms of the surface liquid rate to 200m^3/day for the AICV and 840m^3/day for no AICV cases.

Figure 4-19 shows the plot of cumulative oil production without AICV for the horizontal case (i.e. case-A-2 with dash green line) and the vertical case (i.e. case-A-4 with thick green line). We see that vertical injection of miscible CO_2 injection give a higher cumulative oil rate although it started slowly, it ended up producing 3.3e+07m^3 which is higher than the 3e+07m^3 produced by horizontal injection.

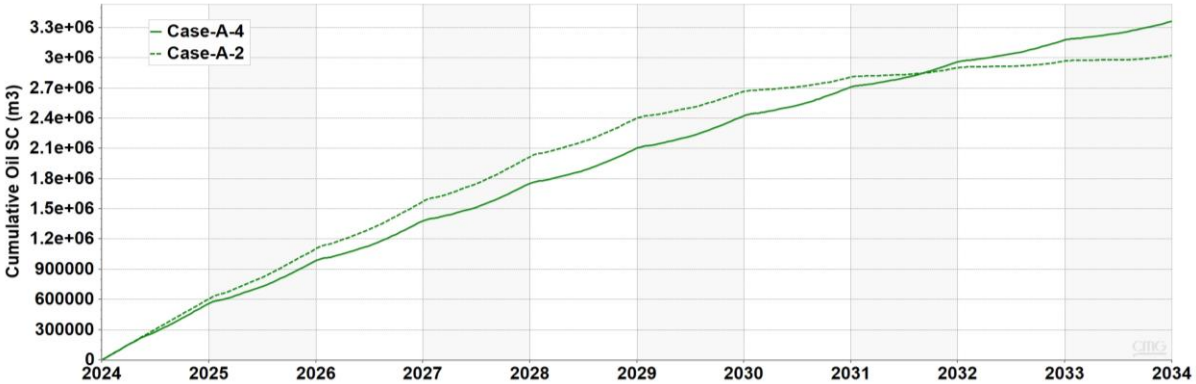

Figure 4-19 The plot of cumulative oil production without AICV for the horizontal case and the vertical case

Figure 4-20 shows the plot of cumulative water production without AICV for the horizontal case (i.e. case-A-2 with dash green blue) and the vertical case (i.e. case-A-4 with thick blue line). We see that vertical injection of miscible CO_2 injection give a lower cumulative water rate although it had the earliest breakthrough, it ended up producing around 2.7e+06m^3 which is lower than the 3e+06m^3 produced by horizontal injection.

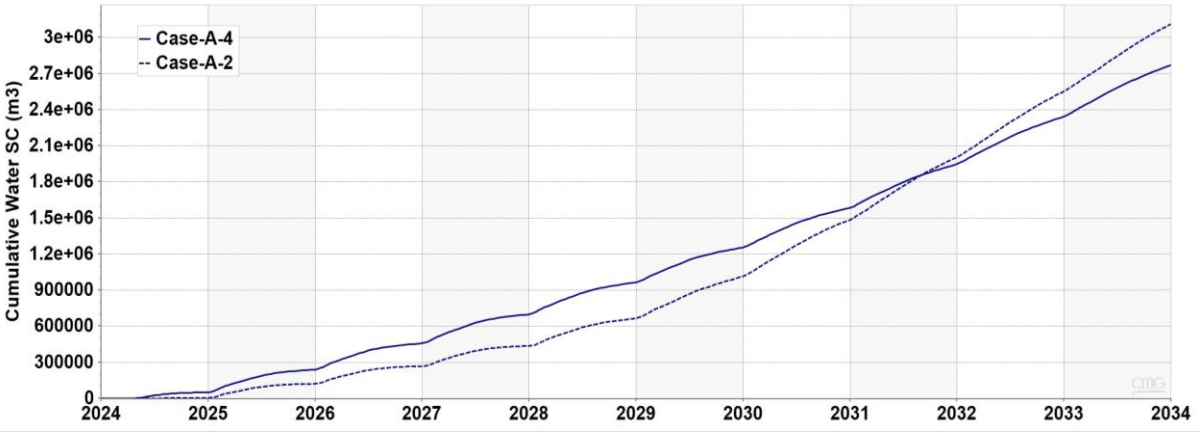

Figure 4-20 The plot of cumulative water production without AICV for the horizontal and the vertical case

In the AICV case, the producer well surface liquid rate constraint was adjusted lower to 200m^3/day because we could not achieve much higher oil production for the vertical producer wells when AICV was installed, this may be due to the length of the vertical producer well which is shorter than the horizontal producer well.

Figure 4-21 shows the plot of cumulative oil production with AICV for the horizontal case (i.e. case-A-1 with dash green line) and the vertical case (i.e. case-A-3 with thick green line). At 200m^3/day, we noticed a slight increase in the cumulative oil of the horizontal producer wells of around 2%.

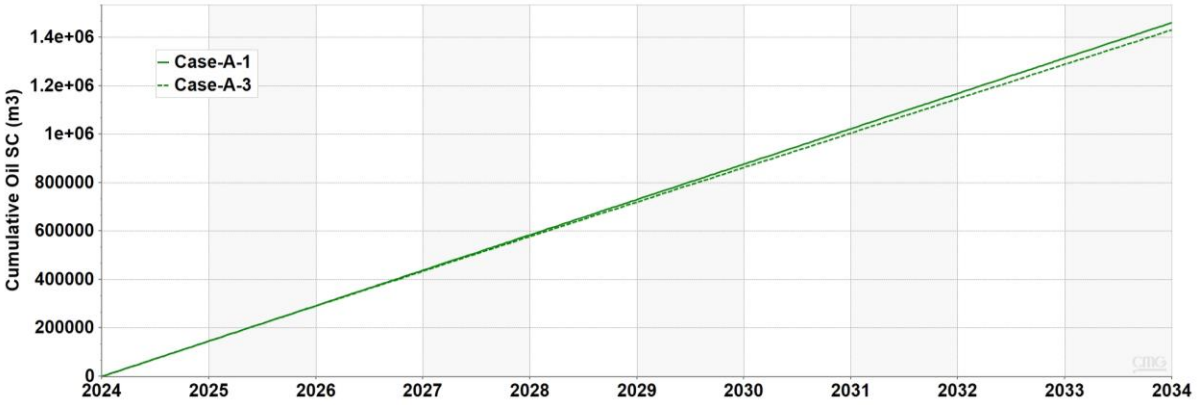

Figure 4-21 The plot of cumulative oil production with AICV for the horizontal and the vertical case

However, with AICV installed there is no water breakthrough for the horizontal miscible CO_2 injection with horizontal producer wells. As shown in Figure 4-22, the vertical injector well with vertical producer wells tends to produce cumulative water of around 3e+04m^3.

Figure 4-22 shows the plot of cumulative water production without AICV for the horizontal case (i.e. case-A-1 with dash blue line) and the vertical case (i.e. case-A-3 with thick blue line).

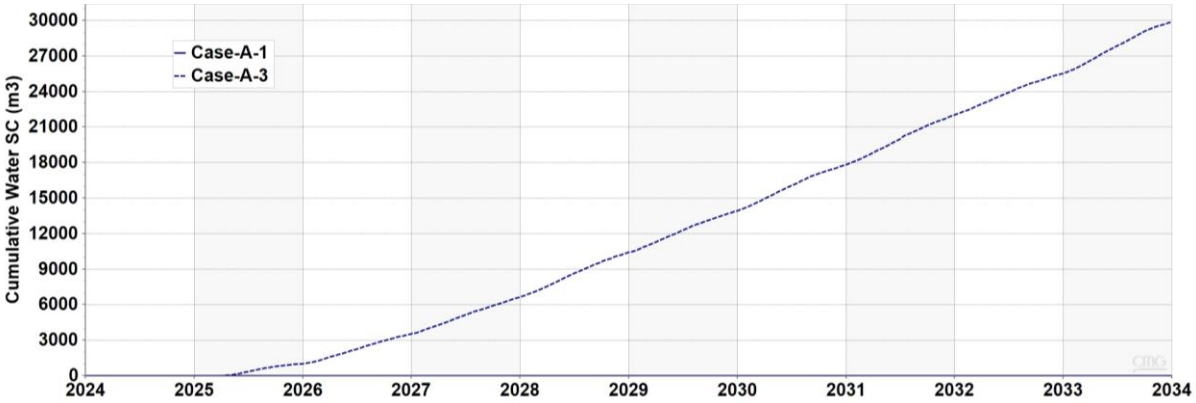

Figure 4-22 The plot of cumulative water production with AICV for the horizontal and the vertical case

Another important observation is the oil saturation from the injector for both vertical and horizontal well with time. Figure 4-23 and Figure 4-24 illustrate the sweeping of oil with time because of the miscible CO_2 injection. At year 2034. From Figure 4-24 we can see that the vertical miscible CO_2 injection has better sweep of the oil with less area of the reservoir left to be covered when compared to horizontal miscible CO_2 injection.

Figure 4-23 shows the oil saturation in the j-k direction view having the injector well perforation in the year 2025 for vertical miscible CO_2 injection (i.e. Case-A-4 on the left-hand-side) and horizontal miscible CO_2 injection (i.e. Case-A-1 on the right-hand-side).

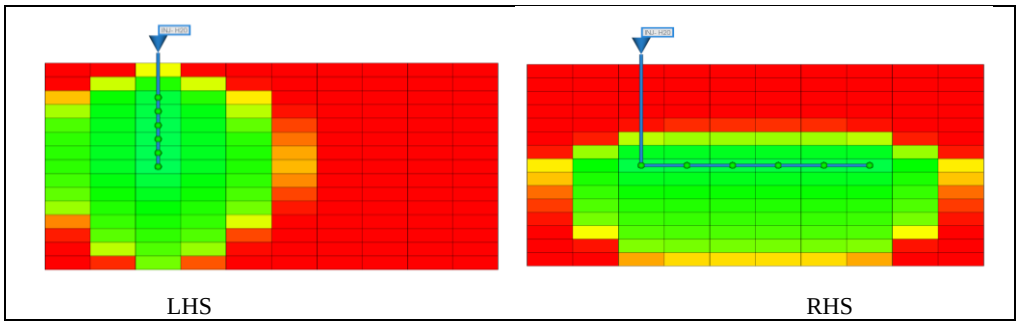

Figure 4-23 The oil saturation at year 2025 of case-A-4 and case-A-1 for the vertical (LHS) and horizontal (RHS) CO2 injection.

Figure 4-24 shows the oil saturation in the j-k direction view having the injector well perforation in the year 2034 for vertical miscible CO_2 injection (i.e. Case-A-4 on the left-hand-side) and horizontal miscible CO_2 injection (i.e. Case-A-1 on the right-hand-side).

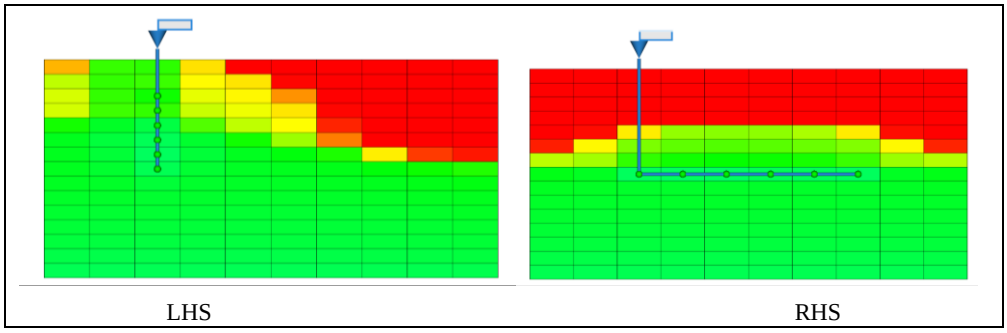

Figure 4-24 The oil saturation at year 2034 of case-A-4 and case-A-1 for the vertical (LHS) and horizontal (RHS) CO2 injection

5 Conclusion

This master's thesis was successful in achieving the objectives and scope. The objectives of the master's thesis performed were literature review on the CO_2-WAG enhanced oil recovery process, simulated model of the miscible CO_2 injection for WAG process on computer modelling group software and evaluation of the performance of the autonomous inflow control valve (AICV) developed by InflowControl AS including sensitivity analysis of the parameters affecting the EOR process.

The results show that the WAG process is a good EOR method over the water-injection because the model simulation achieved increased oil production from 2.4e+06m^3 to 2.7e+06m^3 which is around 12.5% increase. The CMG tool packages such as STARS, Builder and WinProp were very compatible for the miscible CO2 injection. The simulation using CMG provides justifiable results on the AICV performance in accordance with the working principles of the inflow control device as studied in literatures, AICV maintained good oil production while the production of water is decreased from 3e+06m^3 to 9.8e+04m^3 which corresponds to 30 times reduction in water production. Hence, the AICV is a good innovation in the oil industry.

The sensitivity analysis of the simulation results affirms that permeability, well placement, and well spacing have impact on productivity in terms of both oil recovery and water production in the WAG EOR method. The results indicate that permeability increase has a slight increment effect on oil recovery and 50% decrease in water production. The well spacing shows that increasing the distance between the wells will increase the oil recovery and delay the water breaking time. Also, if the wells are too close (possibly less than 20m) recirculation of injected water and CO_2 in the producer wells occurs at the start date. Lastly the well placement shows that vertical injection of miscible CO_2 produces more oil than horizontal injection of miscible CO_2.

In future study, it could be interesting to investigate the optimum perforation location and distance for the CO_2 injector from the producer well which favors maximum oil recovery, reduced operational cost and economic challenges. In addition to a model scenario case of vertical injection with horizontal producer wells, and horizontal injection with vertical producer wells.

References

[1] Bahagio, Danny Natanael Tjahyono. 'AES/PE/13-12 Ensemble Optimization of CO2 WAG EOR', 2013.

[2] Cherian, Bilu V., Edwin S. Stacey, Stephen Bressler, Fabian O. Iwere, Robin Noel Heim, and Shannon Higgins-Borchardt. 'Evaluating Horizontal Well Completion Effectiveness in a Field Development Program'. OnePetro, 2012. https://doi.org/10.2118/152177-MS.

[3] Safi, Razi, Ramesh K. Agarwal, and Subhodeep Banerjee. 'Numerical Simulation and Optimization of CO2 Utilization for Enhanced Oil Recovery from Depleted Reservoirs'. *Chemical Engineering Science* 144 (April 2016): 30–38. https://doi.org/10.1016/j.ces.2016.01.021.

[4] 'Planning and Implementing an EOR Project for the Pre-Salt Lula Field', 8 September 2012. https://www.worldoil.com/magazine/2012/august-2012/supplement/planning-and-implementing-an-eor-project-for-the-pre-salt-lula-field

[5] Halland, Eva Karin, Van Pham, Fridtjof Riis, and Ann-Helen Hansen. 'CO2 for EOR Combined with Storage in the Norwegian North Sea'. *SSRN Electronic Journal*, 2019. https://doi.org/10.2139/ssrn.3365602.

[6] Aakre, Haavard, Vidar Mathiesen, and Britt Moldestad. 'Performance of CO2 Flooding in a Heterogeneous Oil Reservoir Using Autonomous Inflow Control'. *Journal of Petroleum Science and Engineering* 167 (August 2018): 654–63. https://doi.org/10.1016/j.petrol.2018.04.008.

[7] Taghavi Soheila, Seyed Amin Tahami, Haavard Aakre, Nora C.I. Furuvik, and Britt M.E. Moldestad. 'Performance Analysis of Autonomous Inflow Control Valve in a Heterogenous Reservoir Using CO2 Enhanced Oil Recovery'. In *Day 3 Wed, October 18, 2023*, D031S045R002. San Antonio, Texas, USA: SPE, 2023. https://doi.org/10.2118/215153-MS.

[8] Chathurangani, L.B.J., and Britt M. Halvorsen. 'Near Well Simulation of CO2 Injection for Enhanced Oil Recovery (EOR)', 309–18, 2015. https://doi.org/10.3384/ecp15119309.

[9] Berg Iversen, Thomas, Magnus S. Hansen, Sveinung M. Sund, Ole Kristian Vøllestad, Jørgen Bohlin, Nora C. I. Furuvik, and Britt Margrethe Emilie Moldestad. 'Simulation of Oil Production from Heterogeneous North Sea Reservoirs with Inflow Control Using OLGA/Rocx', 196–202, 2017. https://doi.org/10.3384/ecp17138196.

[10] Cherian, Bilu V., Edwin S. Stacey, Stephen Bressler, Fabian O. Iwere, Robin Noel Heim, and Shannon Higgins-Borchardt. 'Evaluating Horizontal Well Completion Effectiveness in a Field Development Program'. OnePetro, 2012. https://doi.org/10.2118/152177-MS.

[11] Zekri, Abdul Razag Y., Shedid A. Shedid, and Reyadh A. Almehaideb. 'Experimental Investigations of Variations in Petrophysical Rock Properties Due to Carbon Dioxide Flooding in Oil Heterogeneous Low Permeability Carbonate Reservoirs'. *Journal of Petroleum Exploration and Production Technology* 3, no. 4 (December 2013): 265–77. https://doi.org/10.1007/s13202-013-0063-0.

[12] Ahmed, Tarek H. *Reservoir Engineering Handbook*. Fifth edition. Cambridge, MA: Elsevier GPP Gulf Professional Publishing, 2019.

[13] Furuvik, Nora, and Britt Halvorsen. 'Simulation of CO2-Distribution in Carbonate Reservoir', 347–55, 2015. https://doi.org/10.3384/ecp15119347.

[14] 'Geologic Storage Is Permanent: An FAQ with Bruce Hill, Ph.D.'. Clean Air Task Force, 9 March 2021. https://www.catf.us/2021/03/geologic-storage-is-permanent-faq/.

[15] Stevens, Scott H., Vello A. Kuuskraa, John Gale, and David Beecy. 'CO2 Injection and Sequestration in Depleted Oil and Gas Fields and Deep Coal Seams: Worldwide Potential and Costs'. *Environmental Geosciences* 8, no. 1 (September 2001): 200–209. https://doi.org/10.1046/j.1526-0984.2001.008003200.x.

[16] Tahami, S. A., B. Dabir, K. Asghari, and A. Shahvaranfard. 'Modeling of Asphaltene Deposition During Miscible CO_2 Flooding'. *Petroleum Science and Technology* 32, no. 18 (17 September 2014): 2183–94. https://doi.org/10.1080/10916466.2010.504937.

[17] Halland, E., F. Riis, W. T. Johansen, I. T. Gjeldvik, and C. Magnus. 'CO2 Storage Atlas of the Norwegian Part of the North Sea', cp. European Association of Geoscientists & Engineers, 2012. https://doi.org/10.3997/2214-4609.20148261.

[18] Cao, Meng, and Yongan Gu. 'Physicochemical Characterization of Produced Oils and Gases in Immiscible and Miscible CO2 Flooding Processes'. *Energy & Fuels* 27, no. 1 (17 January 2013): 440–53. https://doi.org/10.1021/ef301407k.

[19] Moosazadeh, Mohammad, Behnam Keshavarzi, and Cyrus Ghotbi. 'Investigation of the Minimum Miscibility Pressure for Injection of Two Different Gases into Two Iranian Oil Reservoirs: Experimental and Theory'. *The Canadian Journal of Chemical Engineering* 95, no. 5 (2017): 1014–20. https://doi.org/10.1002/cjce.22729.

[20] Zhang, Kaiqiang, Na Jia, Fanhua Zeng, Songyan Li, and Lirong Liu. 'A Review of Experimental Methods for Determining the Oil–Gas Minimum Miscibility Pressures'. *Journal of Petroleum Science and Engineering* 183 (December 2019): 106366. https://doi.org/10.1016/j.petrol.2019.106366.

[21] Adekunle, Olawale, and B. Todd Hoffman. 'Experimental and Analytical Methods to Determine Minimum Miscibility Pressure (MMP) for Bakken Formation Crude Oil'. *Journal of Petroleum Science and Engineering* 146 (1 October 2016): 170–82. https://doi.org/10.1016/j.petrol.2016.04.013.

[22] Randall, T.E., and D.B. Bennion. 'Recent Developments In Slim Tube Testing For Hydrocarbon-Miscible Flood (Hcmf) Solvent Design'. *Journal of Canadian Petroleum Technology* 27, no. 06 (1 November 1988). https://doi.org/10.2118/88-06-02.

[23] Moradi, Ali, Nastaran A. Samani, Amaranath S. Kumara, and Britt M.E. Moldestad. 'Evaluating the Performance of Advanced Wells in Heavy Oil Reservoirs under Uncertainty in Permeability Parameters'. *Energy Reports* 8 (November 2022): 8605–17. https://doi.org/10.1016/j.egyr.2022.06.077.

[24] Kais, Ransis, Vidar Mathiesen, Haavard Aakre, Glenn Woiceshyn, Amr Elarabi, and Ricardo Hernandez. 'First Autonomous Inflow Control Valve AICV Well Completion Deployed in a Field Under an EOR Water & CO2 Injection Scheme'. OnePetro, 2016. https://doi.org/10.2118/181552-MS.

[25] Killie, Rune, Grant J. Paterson, and Thorleif Lager. 'Delivering Automated Reservoir Management with Birth of the First Ever Universal Inflow Control System UICS'. OnePetro, 2021. https://doi.org/10.2118/205868-MS.

[26] 'Product Range | InflowControl'. Accessed 4 May 2024. https://www.inflowcontrol.no/reservoir-solutions/products-.

[27] West, Logan M. 'A Regional Assessment of Residual Oil Zones in the Permian Basin and Their Potential for Carbon Dioxide Capture Usage and Storage'. *Energy Procedia*, 12th International Conference on Greenhouse Gas Control Technologies, GHGT-12, 63 (1 January 2014): 7884–90. https://doi.org/10.1016/j.egypro.2014.11.824.

[28] Copenhagen, Calsep. '#23 Characterization of CO2 Rich Fluids | Calsep', 18 November 2022. https://www.calsep.com/23-characterization-of-co2-rich-fluids/.

[29] Oomole, O., and J. S. Osoba. 'Carbon Dioxide - Dolomite Rock Interaction During CO2 Flooding Process'. OnePetro, 1983. https://doi.org/10.2118/83-34-17.

Appendices

Appendix A: Task Description

Appendix B: The Relative Permeability Curve

Appendix A

Task Description

FMH606 Master's Thesis

Title: CO_2 Enhanced Oil Recovery in Reservoirs with Advanced Wells; Simulations and Sensitivity Analysis

USN supervisor: Associate professor Nora C.I. Furuvik and Soheila Taghavi Hosnaroudi

Co-Supervisor:

External partner: InflowControl AS

Task description:

The objectives of the research project can be achieved by completing the following tasks:

1. Comprehensive literature study
   - Reservoir rock and fluid properties
   - EOR methods by focusing on CO_2 water alternating gas (WAG)-EOR
   - Miscible CO_2 EOR mechanism and potentials
   - Advanced wells and their impact on increased EOR
   - CO_2 and reservoir fluids characteristics
2. Modelling and Simulation
   - Simulate oil production by using advanced wells completed with different flow control technologies such as autonomous inflow control valve (AICV) and inflow control device (ICD).
   - Evaluate the performance of different flow control technologies in advanced wells.
   - Sensitivity analysis of the parameters affecting the CO_2 EOR process in combination with advanced wells.
3. If time allows to prepare a paper based on the obtained results for the next SIMS conference is highly appreciated.

Student category: EET and PT. It is an advantage that the student has good knowledge within fluid dynamics.

Is the task suitable for online students (not present at the campus)? No

Practical arrangements:

Necessary software will be provided by USN.

Supervision:

As a general rule, the student is entitled to 15-20 hours of supervision. This includes necessary time for the supervisor to prepare for supervision meetings (reading material to be discussed, etc.).

Signatures:

Supervisor (date and signature):

Student (write clearly in all capitalized letters):

Student (date and signature):

Appendix B

The Relative Permeability Curve

Table B-1 The relative permeability data for the water-oil.

Sw	Krw	Krow
0.250	0.000	0.900
0.283	0.001	0.742
0.316	0.005	0.603
0.349	0.011	0.483
0.383	0.019	0.380
0.416	0.029	0.292
0.449	0.042	0.220
0.482	0.057	0.160
0.515	0.075	0.113
0.548	0.095	0.075
0.581	0.117	0.047
0.614	0.142	0.027
0.648	0.169	0.014
0.681	0.198	0.006
0.714	0.230	0.002
0.747	0.264	0.000
0.780	0.300	0.000

Table B-2 The relative permeability data for the gas-liquid.

Sl	Krg	Krog
0.550	0.300	0.000
0.575	0.247	0.000
0.600	0.201	0.001
0.625	0.161	0.004
0.650	0.127	0.010
0.675	0.097	0.019
0.700	0.073	0.033
0.725	0.053	0.053
0.750	0.038	0.079
0.775	0.025	0.113
0.800	0.016	0.154
0.825	0.009	0.205
0.850	0.005	0.267
0.875	0.002	0.339
0.900	0.001	0.423
0.925	0.000	0.521
0.950	0.000	0.632
0.975	0.000	0.758
1.000	0.000	0.900